

Predictive fermion mass matrix *Ansätze* in nonsupersymmetric SO(10) grand unification

N. G. Deshpande and E. Keith

Institute of Theoretical Science, University of Oregon, Eugene, Oregon 97403-5203

(Received 15 February 1994)

We investigate the status of predictive fermion mass *Ansätze* in nonsupersymmetric SO(10) grand unification which make use of the grand unification scale conditions $m_e = m_d/3$, $m_\mu = 3m_s$, and $|V_{cb}| = \sqrt{m_c/m_t}$ in nonsupersymmetric SO(10) grand unification. The gauge symmetry below an intermediate symmetry-breaking scale M_I is assumed to be that of the standard model with either one Higgs doublet or two Higgs doublets. We find in both cases that a maximum of five standard model parameters may be predicted within 1σ experimental ranges. We find that the standard model scenario predicts the low energy $|V_{cb}|$ to be in a range which includes its experimental midvalue 0.044 and which for a large top mass can extend to lower values than the range resulting in the supersymmetric case. In the two Higgs standard model case, we identify the regions of parameter space for which unification of the bottom quark and τ lepton Yukawa couplings is possible at grand unification scale. In fact, we find that unification of the top, bottom, and τ Yukawa couplings is possible with the running b -quark mass within the 1σ preferred range $m_b = 4.25 \pm 0.1$ GeV provided $\alpha_{3c}(M_Z)$ is near the low end of its allowed range. In this case, one may make six predictions which include $|V_{cb}|$ within its 90% confidence limits. However unless the running mass $m_b > 4.4$ GeV, third generation Yukawa coupling unification requires the top mass to be greater than 180 GeV. We compare these nonsupersymmetric cases to the case of the minimal supersymmetric standard model embedded in the SO(10) grand unified group. We also give an example of a possible mechanism, based on induced vacuum expectation values and a broken $U(1)^3$ symmetry for generating the observed hierarchy of masses and a mass matrix texture.

PACS number(s): 12.15.Ff, 12.10.Dm

I. INTRODUCTION

Recently, much attention has been given to the successes of predictive *Ansätze* [1–4] for the fermion sector of the standard model (SM). Although originally fermion sector *Ansätze* [5–9] were proposed for and used in the nonsupersymmetric SM [7, 8] and SU(5) and SO(10) [10] grand unified models, recent attention has focused on the case of the minimal supersymmetric standard model (MSSM) contained in supersymmetric SO(10). One reason for using an *Ansatz* in the context of a grand unified theory is that in these theories the masses of the down quarks and the charged leptons are necessarily related. This gives the possibility of increased predictive ability which, for example, may be realized in the Georgi-Jarlskog (GJ) mechanism [6] which has at the grand unification scale $m_e = m_d/3$, $m_\mu = 3m_s$, and $m_\tau = m_b$. Also, there is the possibility of relating the up quark mass matrix to the down quark mass matrix [11]. This happens when the up and down quarks receive their masses from the same Yukawa couplings or higher dimensional operators in the context of the grand unified theory. It has also been shown [1, 4] that by applying an *Ansatz* with $|V_{cb}| = \sqrt{m_c/m_t}$ at the grand unification scale, and requiring the zero terms in the mass matrices to be protected by some symmetries above the grand unification scale, $|V_{cb}|$ is predicted to be within or close to the upper end of the 1σ experimental range without requiring m_t to be too large. SO(10) [or a group such as

E_6 containing SO(10)] is the chosen group because then, unlike SU(5), the mass matrices can be automatically symmetric, neutrinos may be given small masses with mixing to solve the solar neutrino problem, and there are useful relations between the mass matrices [1]. In the Dimopoulos-Hall-Raby (DHR) formulation [1], the MSSM with gauge coupling unification is chosen because by requiring unification of gauge couplings and the supersymmetry (SUSY) effective scale parameter M_S to be in the proximity of 1 TeV, as is needed for SUSY to solve the fine-tuning problem, one can predict $\alpha_{3c}(M_Z)$ to be within its experimentally determined range from the experimentally well determined parameters α and $\sin\theta_W$ [12].

Although the fermion mass *Ansätze* in SUSY SO(10) have so far worked quite well, there is, as of yet, no evidence for SUSY and one may wish to compare the predictions and predictive ability of *Ansätze* with SUSY to those without SUSY. This is useful not only because we do not know whether SUSY exists, but also because many parameters of the fermion mass and the quark mixing sector have not yet been determined with great precision; so we cannot yet be confident of the success of the predictions of any particular scheme. The first comprehensive discussion of the predictions in the fermion sector of an *Ansatz* was done in Ref. [1] for the case of MSSM contained in SUSY SO(10). Only recently have the low energy data (LED) been precise enough to give a reasonable test of the predictions of an *Ansatz*. In this paper, we

will look at fermion mass *Ansätze* in non-SUSY SO(10) grand unification in terms of current LED.

As in Ref. [1], we take the *Ansatz* at unification scale and assume that some, as yet, unspecified symmetries enforce the zero terms in the fermion mass matrices at that scale. One expects that such symmetries originate in a theory that is realized at scales equal to or greater than the grand unification scale and that these symmetries are broken at the grand unification scale, which allows the zero terms in the fermion mass matrices to develop finite values from renormalization group effects. We will suggest an example of such a scenario in Sec. VI of this paper. Without the intention of examining all possible textures of fermion mass matrices, we will assume an up quark mass matrix based on the Fritzsch *Ansatz* [5] and down and charged lepton mass matrices based on the Georgi-Jarlskog *Ansatz* [6]. *Ansätze* of this general form have been used extensively in the literature.

Although SUSY SO(10) can break to the MSSM in only one step, non-SUSY SO(10) in general needs at least two steps to break to the SM. Typically, in two-step breaking of SO(10) to the SM with Higgs particles taking masses according to the survival hypothesis as given by the principal of minimal fine-tuning [13], the intermediate scale $M_I \sim 10^9\text{--}10^{11}$ GeV and the unification scale $M_U \sim 10^{16}$ GeV [14]. The allowed single intermediate scale gauge symmetries are the four groups $\{2_L 2_R 4_C\}$, $\{2_L 2_R 4_C P\}$, $\{2_L 2_R 1_{B-L} 3_c\}$, and $\{2_L 2_R 1_{B-L} 3_c P\}$, where P refers to D parity not having been broken and where, for example, $\{2_L\}$ refers to $SU(2)_L$. [Only in SUSY SO(10) is $SU(5) \otimes U(1)$ as an intermediate symmetry group possible.] Another possibility, pointed out recently, is that if threshold effects are not minimized [15] according to the survival hypothesis, but to the contrary superheavy Higgs particles not contributing to proton decay are allowed to vary below a SM coupling unification scale by a factor that can be as high as 10, then it is possible for $M_U/M_I \leq 30$ [16]. Like the SUSY case, this scheme makes one low energy prediction in the gauge sector from two inputs. It predicts $\alpha_{3c}(M_Z)$ in the range of 0.119–0.125. In our paper, we will look at cases where SO(10) breaks at a scale M_U via the vacuum expectation value (VEV) which is contained in a **210** [17] representation Higgs field to the gauge symmetry $\{2_L 2_R 4_C\}$ and next at a scale $M_I \sim 10^{11}$ or 10^{14} GeV to the SM. Further, we will assume that the VEV which breaks the gauge symmetry $\{2_L 2_R 4_C\}$ to the SM is contained in an $SU(2)_R$ triplet of a **126** representation Higgs field. This gives the right-handed neutrinos Majorana masses. As usual, we use the VEV of a complex **10** representation Higgs field for the electroweak symmetry breaking. Even though the scheme of Ref. [16] requires high values of $\alpha_{3c}(M_Z)$, we will consider $\alpha_{3c}(M_Z) = 0.118 \pm 0.007$ for both $M_I \sim 10^{11}$ and $M_I \sim 10^{14}$ GeV.

Below the scale M_I , we consider two possibilities: one that the effective theory is the conventional one-Higgs-doublet SM and the second possibility that the effective theory is the two-Higgs-doublet standard model (2HSM). The reason we are interested in the 2HSM is that both the unification of the Yukawa couplings of the bottom quark and τ lepton and unification of all three third-generation

SM Yukawa couplings are possible in the 2HSM, while as we will see in the SM case the unification of the Yukawa couplings of the bottom quark and τ lepton is not feasible.

The rest of this paper is organized in the following manner. In the next section, we will discuss the renormalization group equations (RGE's) of the fermion sector parameters and the gauge couplings. After that, we review the basic results of implementing the GJ *Ansatz* in the MSSM. We do this so that we may later compare the results for the two cases without SUSY to the case with SUSY. In Sec. IV, we will discuss the case of a fermion mass *Ansatz* when between the scales of m_t and M_I the effective theory is the SM. In Sec. V, we discuss the case of a fermion mass *Ansatz* when instead of the SM the effective theory below M_I is the 2HSM. Next, we give an example of a possible explanation of fermion generation mass hierarchy and flavor symmetries by use of induced VEV's [18] in superheavy Higgs fields and a broken $U(1)^3$ symmetry. In the final section, we summarize the paper.

II. RGE'S AND LED

Here, we remind the reader of how Yukawa couplings evolve in the SM gauge symmetry $\{1_Y 2_L 3_c\}$ in the one-loop approximation [19], which we will use. Let \mathbf{U} , \mathbf{D} , and \mathbf{E} be the 3×3 Yukawa matrices in generation space for the up and down quarks, and the charged leptons, respectively. In the SM, we have the Yukawa couplings

$$\mathcal{L}_Y = \bar{q}_L \mathbf{U} \tilde{\phi} u_R + \bar{q}_L \mathbf{D} \phi d_R + \bar{l}_L \mathbf{E} \phi e_R + \text{H.c.} \quad (1)$$

In the MSSM and in the 2HSM we have

$$\mathcal{L}_Y = \bar{q}_L \mathbf{U} \phi_u u_R + \bar{q}_L \mathbf{D} \phi_d d_R + \bar{l}_L \mathbf{E} \phi_d e_R + \text{H.c.}, \quad (2)$$

where $\langle |\phi_u| \rangle = \kappa_u$ and $\langle |\phi_d| \rangle = \kappa_d$ with $\sqrt{|\kappa_u|^2 + |\kappa_d|^2} = \kappa = 174$ GeV and $\kappa_u/\kappa_d \equiv \tan\beta$. The one-loop RGE's for these couplings are

$$16\pi^2 \frac{d\mathbf{U}}{dt} = \left[\text{Tr}(3\mathbf{U}\mathbf{U}^\dagger + 3a\mathbf{D}\mathbf{D}^\dagger + a\mathbf{E}\mathbf{E}^\dagger) + \frac{3}{2}(b\mathbf{U}\mathbf{U}^\dagger + c\mathbf{D}\mathbf{D}^\dagger) - \sum_i c_i^{(u)} g_i^2 \right] \mathbf{U}, \quad (3)$$

$$16\pi^2 \frac{d\mathbf{D}}{dt} = \left[\text{Tr}(3a\mathbf{U}\mathbf{U}^\dagger + 3\mathbf{D}\mathbf{D}^\dagger + \mathbf{E}\mathbf{E}^\dagger) + \frac{3}{2}(b\mathbf{D}\mathbf{D}^\dagger + c\mathbf{U}\mathbf{U}^\dagger) - \sum_i c_i^{(d)} g_i^2 \right] \mathbf{D}, \quad (4)$$

$$16\pi^2 \frac{d\mathbf{E}}{dt} = \left[\text{Tr}(3a\mathbf{U}\mathbf{U}^\dagger + 3\mathbf{D}\mathbf{D}^\dagger + \mathbf{E}\mathbf{E}^\dagger) + \frac{3}{2}b\mathbf{E}\mathbf{E}^\dagger - \sum_i c_i^{(e)} g_i^2 \right] \mathbf{E}, \quad (5)$$

with $t = \ln \mu$,

$$\text{SM: } (a, b, c) = (1, 1, -1); \quad (6)$$

$$\text{2HSM: } (a, b, c) = \left(0, 1, \frac{1}{3}\right); \quad (7)$$

$$\text{MSSM: } (a, b, c) = \left(0, 2, \frac{2}{3}\right); \quad (8)$$

and

$$\text{SM, 2HSM: } c_i^{(u)} = \left(\frac{17}{20}, \frac{9}{4}, 8\right), c_i^{(d)} = \left(\frac{1}{4}, \frac{9}{4}, 8\right), \quad (9)$$

$$c_i^{(e)} = \left(\frac{9}{4}, \frac{9}{4}, 0\right);$$

$$\text{MSSM: } c_i^{(u)} = \left(\frac{13}{15}, 3, \frac{16}{3}\right), c_i^{(d)} = \left(\frac{7}{15}, 3, \frac{16}{3}\right), \quad (10)$$

$$c_i^{(e)} = \left(\frac{9}{5}, 3, 0\right).$$

In computing the evolution of the gauge couplings, we will use a two-loop analysis but we will ignore the small effects of the Yukawa couplings on their running. The two-loop equations, which we numerically integrate, are of the form

$$\mu \frac{\partial \alpha_i^{-1}(\mu)}{\partial \mu} = -\frac{1}{2\pi} \left(b_i + \frac{b_{ij}}{4\pi} \alpha_j(\mu) \right). \quad (11)$$

The one-loop coefficients b_i are

$$\text{SM: } (b_1, b_2, b_3) = \left(\frac{41}{10}, \frac{-19}{6}, -7\right); \quad (12)$$

$$\text{2HSM: } (b_1, b_2, b_3) = \left(\frac{21}{5}, 3, -7\right); \quad (13)$$

$$\text{MSSM: } (b_1, b_2, b_3) = \left(\frac{33}{5}, 1, -3\right). \quad (14)$$

The two-loop coefficients b_{ij} can be extracted from Ref. [20]. We use gauge couplings normalized so as to become equal at the scale M_U . We use the following gauge sector inputs [21]:

$$\begin{aligned} \alpha^{-1}(M_Z) &= 127.9, \\ \alpha_{3c}(M_Z) &= 0.118 \pm 0.007, \\ \tilde{x}(M_Z) &= 0.2326, \\ M_Z &= 91.187 \pm 0.007 \text{ GeV}, \end{aligned} \quad (15)$$

with

$$\alpha_{1Y}^{-1}(M_Z) = \frac{3}{5} \frac{1 - \tilde{x}}{\alpha(M_Z)}, \quad (16)$$

$$\alpha_{2L}^{-1}(M_Z) = \frac{\tilde{x}}{\alpha(M_Z)}, \quad (17)$$

and we have used the experimental midvalues for $\alpha(M_Z)$ and $\tilde{x} \equiv \sin^2 \theta_W M_{(\overline{\text{MS}})}$, where $\overline{\text{MS}}$ denotes the modified minimal subtraction scheme.

As in Ref. [1], we numerically integrate α_1 , α_2 , and α_3 from M_Z up to a scale μ_t which is in the vicinity of where we expect to find the top mass m_t . Between $\mu = M_Z$ and $\mu = \mu_t$, we use the two-loop SM gauge evo-

lution with one-loop threshold corrections for $m_t = \mu_t$ to find α_{1Y} , α_{2L} , and α_{3c} at the scale $\mu = \mu_t$. From $\mu = \mu_t$ down to a particular fermion's running mass for m_b , m_c , or charged leptons or down to 1 GeV for the less massive quarks, we calculate the running of its mass according to three-loop QCD [22] and one-loop QED effects. Cabibbo-Kobayashi-Maskawa (CKM) parameters are evaluated at the scale μ_t . Of course, we always use the effective theory where all fermions more massive than the scale of interest have been integrated out. These effects are represented by $m_i = m_i(\mu_t) \eta_i$. In this paper, we take $\mu_t = 180$ GeV and use $m_b = 4.25$ GeV and $m_c = 1.27$ GeV in calculating η_b and η_c , respectively. We find $\alpha_1^{-1}(\mu_t) = 58.51$, $\alpha_2^{-1}(\mu_t) = 30.15$, $\alpha_3^{-1}(\mu_t) = 9.30_{+0.054}^{-0.047}$, and

$$\begin{aligned} \eta_b &= 1.53_{-0.06}^{+0.07}, \\ \eta_c &= 2.09_{-0.19}^{+0.27}, \\ \eta_s = \eta_d &= 2.36_{-0.29}^{+0.53}, \\ \eta_u &= 2.38_{-0.30}^{+0.52}, \\ \eta_e \approx \eta_\mu \approx \eta_\tau &= 1.015. \end{aligned} \quad (18)$$

We are interested in the low energy fermion masses, the CKM quark mass mixing matrix elements $V_{\alpha\beta}$, and the Jarlskog CP violation parameter J . In the approximation that we use the one-loop Yukawa RGE's, ignore terms $O(\lambda_c^2)$ or smaller where λ_i is the Yukawa coupling of fermion i , assume only small mixing between generations of quarks, and set $\eta_t = 1$, the exact solutions for the LED in terms of the same parameters at an intermediate scale μ_I are [23, 24]

$$m_t(m_t) = m_t(\mu_I) A_u e^{-(3+\frac{3}{2}b)I_t - (3a+\frac{3}{2}c)I_b - aI_\tau}, \quad (19)$$

$$m_b(m_b) = m_b(\mu_I) \eta_b A_d e^{-(3a+\frac{3}{2}c)I_t - (3+\frac{3}{2}b)I_b - I_\tau}, \quad (20)$$

$$m_\tau(m_\tau) = m_\tau(\mu_I) \eta_\tau A_d e^{-3aI_t - 3I_b - (1+\frac{3}{2}b)I_\tau}, \quad (21)$$

$$m_c(m_c) = m_c(\mu_I) \eta_c A_u e^{-3I_t - 3aI_b - aI_\tau}, \quad (22)$$

$$m_i(m_i) = m_i(\mu_I) \eta_\mu A_e e^{-3aI_t - 3I_b - I_\tau} \quad (\text{for } i = \mu, e), \quad (23)$$

$$m_i(1 \text{ GeV}) = m_i(\mu_I) \eta_s A_d e^{-3aI_t - 3I_b - I_\tau} \quad (\text{for } i = s, d), \quad (24)$$

$$m_u(1 \text{ GeV}) = m_u(\mu_I) \eta_u A_u e^{-3I_t - 3aI_b - aI_\tau}, \quad (25)$$

$$|V_{\alpha\beta}(m_t)| = |V_{\alpha\beta}(\mu_I)| e^{\frac{3}{2}cI_t + \frac{3}{2}cI_b} \quad (\text{for } \alpha\beta = ub, cb, tb, ts), \quad (26)$$

$$|V_{\alpha\beta}(m_t)| = |V_{\alpha\beta}(\mu_I)| \quad (\text{for other } \alpha\beta), \quad (27)$$

$$J(m_t) = J(\mu_I) e^{3cI_t + 3cI_b}, \quad (28)$$

where the effect of third-generation Yukawa couplings on the Yukawa evolution is given as [11]

$$I_i = \int_{\mu_t}^{\mu_I} \left(\frac{\lambda_i(\mu)}{4\pi} \right)^2 d(\ln \mu), \quad (29)$$

and the effect of gauge couplings on Yukawa evolution is given as [24]

$$A_\alpha = \exp \left[\frac{1}{16\pi^2} \int_{\ln \mu_t}^{\ln \mu_I} \sum_i c_i^{(\alpha)} g_i^2(\mu) d(\ln \mu) \right]. \quad (30)$$

In the one-loop approximation for the gauge RGE's, A_α becomes

$$A_\alpha = \prod \left(\frac{\alpha_{i_I}}{\alpha_{i_t}} \right)^{\frac{c_i^{(\alpha)}}{2b_i}}. \quad (31)$$

In the SM or in the 2HSM or MSSM when $\tan\beta$ is small, it is a very good approximation to ignore terms $O(\lambda_b^2)$ in the Yukawa coupling evolution equations, in which case [24]

$$e^{I_t} = [1 + \lambda_{t_I}^2 K_u]^{\frac{1}{6+3b}}, \quad (32)$$

where $\lambda_{t_I} = \lambda_t(M_I)$ and

$$K_u = \frac{6 + 3b}{16\pi^2} \int_{\ln \mu_t}^{\ln \mu_I} \exp \left[\frac{1}{8\pi^2} \int_{\ln \mu}^{\ln \mu_I} \sum_i c_i^{(\alpha)} g_i^2(\mu') \times d(\ln \mu') \right] d(\ln \mu). \quad (33)$$

In Table I, we give the values for the A_α 's and the K_u 's for the SM and the 2HSM. We show two different cases for the situation where the effective theory below the scale M_I is the SM. In the SM case (a) $M_I = 10^{10.94}$ GeV, and in the SM case (b) $M_I = 10^{14}$ GeV. In the case where the effective theory between μ_t and M_I is the 2HSM, we use $M_I = 10^{11.28}$ GeV. Note that the A_α 's and the K_u 's in the SM case (a) and the 2HSM case have very similar values. For the sake of comparison, we also show the A_α 's and K_u for the case when the effective theory above the scale $\mu_t = 180$ GeV is the MSSM. In this case, the upper bound of integration in the A_α 's and K_u is the gauge coupling unification scale M_U . The strong coupling constant $\alpha_{3c}(M_Z) = 0.121$ is determined by requiring gauge coupling unification to be achieved with α and $\sin\theta_W$ as inputs.

In Table I, we also show the ratio A_d/A_e in the different cases because the ratio of the masses of the down quarks to the masses of the charged leptons is proportional to A_d/A_e . Note that this ratio is highest in the MSSM scenario. In the SM case (b) this ratio is higher than in the other two non-SUSY cases because the $SU(4)_C$ gauge symmetry is broken at M_I , which for SM case (b) is larger than for the other two non-SUSY scenarios considered.

We can use the A_u 's and K_u 's of Table I to find the infrared quasifixed point of the top quark [25]. When

$\lambda_t \gg \lambda_b$,

$$\lambda_t = \frac{AA_u}{\sqrt{1 + A^2 K_u}}, \quad (34)$$

where A is the top quark Yukawa coupling at the scale M_I for the non-SUSY cases and at M_U for the MSSM case. In the limit of a large A , one finds $\lambda_t \approx A_u/\sqrt{K_u}$. Therefore in the MSSM when $\sin\beta \approx 1$ and $\lambda_t \gg \lambda_b$, $(A_u/\sqrt{K_u})\kappa$ is the infrared quasifixed point of the top quark. For the MSSM case, one finds that the fixed point is 194 GeV. This gives an upper bound for the running mass m_t for any $\tan\beta$.

However, when an intermediate breaking scale M_I exists, A has an upper bound from the following equation which is valid when the intermediate gauge symmetry is $\{2_L 2_R 4_C\}$:

$$A = \frac{\lambda_{t_U} A_f}{\sqrt{1 + \lambda_{t_U}^2 K_f}}, \quad (35)$$

where we have defined the effect of the intermediate scale gauge couplings g_{2L} , g_{2R} , and g_{4C} on the Yukawa coupling evolution of all fermions as

$$A_f = \exp \left[\frac{1}{16\pi^2} \int_{\ln \mu_t}^{\ln \mu_I} \sum_i c_i^{(f)} g_i^2(\mu) d(\ln \mu) \right], \quad (36)$$

and defined the analogue of K_u as

$$K_f = \frac{3}{4\pi^2} \int_{\ln \mu_t}^{\ln \mu_I} \exp \left[\frac{1}{8\pi^2} \int_{\ln \mu}^{\ln \mu_I} \sum_i c_i^{(f)} g_i^2(\mu') \times d(\ln \mu') \right] d(\ln \mu), \quad (37)$$

with

$$c_i^{(f)} = \left(\frac{9}{4}, \frac{9}{4}, \frac{45}{4} \right), \quad (38)$$

and λ_{t_U} is the top quark Yukawa coupling at M_U . Equation (35) is the solution to the intermediate scale equation

$$16\pi^2 \frac{d \ln \lambda_t}{dt} = \left(6\lambda_t^2 - \sum_i c_i^{(f)} g_i^2 \right). \quad (39)$$

For the SM case (a), we find the fixed point to be $223 \pm$

TABLE I. In this table, we show the gauge contribution factors A_α , defined in Eq. (30), the quantity K_u , defined in Eq. (33), and the ratio $R_d = \frac{A_d}{A_e}$. In the first three cases listed, we assume that the $SO(10)$ grand unified group breaks to the gauge group $\{2_L 2_R 4_C\}$ at the scale M_U , and then the gauge symmetry $\{2_L 2_R 4_C\}$ is broken to either the SM or the 2HSM at the scale M_I . In the SM case (a), the SM case (b), and the 2HSM case, we have assumed $M_I = 10^{10.93}$ GeV, $M_I = 10^{14}$ GeV, and $M_I = 10^{11.28}$ GeV, respectively. For the purpose of comparison, we also give the results for the MSSM with the assumptions of gauge coupling unification (for which we ignore threshold effects) and $m_t \approx M_S = 180$ GeV used to determine $\alpha_{3c}(M_Z) = 0.121$.

Scenario	A_u	A_d	A_e	K_u	$R_d = \frac{A_d}{A_e}$
SM case (a)	2.27 ± 0.05	2.23 ± 0.05	1.19	2.51 ± 0.05	1.87 ± 0.05
SM case (b)	2.69 ± 0.06	2.62 ± 0.06	1.26	3.98 ± 0.08	2.08 ± 0.04
2HSM	2.32 ± 0.05	2.28 ± 0.05	1.20	2.66 ± 0.05	1.90 ± 0.04
MSSM	3.45	3.36	1.50	9.55	2.24

3 GeV. For the SM case (b), we find $\kappa A_u/\sqrt{K_u} = 235 \pm 4$ GeV. For the 2HSM case, we find the upper bound of the top running mass to be 225 ± 3 GeV. As is well known, without SUSY the fixed point of the top quark is clearly higher than that allowed for by examination of electroweak data [26].

We now should consider the relations between m_b and m_τ in the three cases. They are

$$\frac{m_b}{m_\tau} = \frac{\lambda_{bU}}{\lambda_{\tau U}} \frac{\eta_b}{\eta_\tau} \frac{A_d}{A_e} e^{-\frac{3}{2}cI_t - \frac{3}{2}bI_b + \frac{3}{2}bI_\tau} \quad (40)$$

$$= \frac{\lambda_{bU}}{\lambda_{\tau U}} \frac{\eta_b}{\eta_\tau} \frac{A_d}{A_e} e^{\frac{3}{2}I_t - \frac{3}{2}I_b + \frac{3}{2}I_\tau} \quad (\text{SM}) \quad (41)$$

$$= \frac{\lambda_{bU}}{\lambda_{\tau U}} \frac{\eta_b}{\eta_\tau} \frac{A_d}{A_e} e^{-\frac{1}{2}I_t - \frac{3}{2}I_b + \frac{3}{2}I_\tau} \quad (2\text{HSM}) \quad (42)$$

$$= \frac{\lambda_{bU}}{\lambda_{\tau U}} \frac{\eta_b}{\eta_\tau} \frac{A_d}{A_e} e^{-I_t - 3I_b + 3I_\tau} \quad (\text{MSSM}) \quad (43)$$

where the subscript U on a parameter denotes its value at unification scale. The $SU(3)_c$ gauge contribution by itself would make m_b undesirably large for the case of bottom- τ Yukawa coupling unification with the requirement $m_\tau = 1.784$ GeV. Inclusion of the top quark's contribution makes the situation worse in the SM, but improves it in the 2HSM and MSSM.

In the SM case, the ratio m_b/m_τ increases with top quark mass. This ratio also increases with the $SU(4)_C$ -breaking scale M_I . According to Ref. [27] in which the M_I scale relation $m_b = m_\tau$ is discussed for non-SUSY models, either the running mass m_b must be greater than 4.35 GeV or the top pole mass must be lighter than 80 GeV for M_I to be consistent with $SO(10)$ grand unification. Using a two-loop gauge analysis with the recent 1σ lower bound on $\alpha_{3c}(M_Z)$ of 0.111 and the recent lower bound on the top pole mass of 130 GeV, we find even tighter constraints. From the previously given RGE's, one may find the following expression for the top quark running mass:

$$m_t = \sqrt{1 - \left(\frac{\tau}{b}\right)^6} \frac{A_u}{\sqrt{K_u}} \kappa, \quad (44)$$

with $\tau \equiv m_\tau/\eta_\tau A_e$ and $b \equiv m_b/\eta_b A_d$. For example, if we assume the high value 4.8 GeV for m_b and the low values of $10^{10.85}$ GeV for M_I and 0.111 for $\alpha_{3c}(M_Z)$, we calculate $\eta_b = 1.41$, $\eta_\tau = 1.015$, $A_u = 2.27$, $A_d = 2.23$, $A_e = 1.19$, and $K_u = 2.52$ for the choice of $\mu_t = 130$ GeV. This predicts a top pole mass of about 110 GeV. In fact, even if we ignored the effect of the top quark on this ratio, still the running mass of the bottom quark would be predicted to be $m_\tau \eta_b A_d / \eta_\tau A_e = 4.6$ GeV, which is fairly large.

To get a bottom quark mass within a desirable range, we are forced into using two Yukawa couplings to give mass to the bottom and τ fermions in the one-Higgs-doublet case. One coupling must be to a **10** representation Higgs field and the other to a $\overline{\mathbf{126}}$ representation Higgs field. (Remember that, unlike a coupling to a **10**, couplings to $\overline{\mathbf{126}}$'s contribute to lepton Dirac masses relative to quark masses with a factor of the Clebsch coefficient of -3 .) We assume the entire bidoublet of the $\overline{\mathbf{126}}$

representation Higgs field to have a mass of the order of M_U and to contribute to the fermion masses through a VEV induced from the VEV of the **10** representation Higgs field [18].

On the other hand, in the 2HSM and the MSSM when we input $m_\tau = 1.784$ and require the unification scale condition $m_b = m_\tau$, the ratio m_b/m_τ decreases with increasing m_t as can be seen from the exponents in Eqs. (42) and (43). Bottom- τ Yukawa coupling unification has proved successful in the MSSM. We will see later that this is also possible in the 2HSM, although the fit is not as attractive. This is because the ability of the top quark Yukawa coupling to keep the ratio m_b/m_τ from becoming too large is less in the 2HSM than in the MSSM.

Since we are interested in matrices of the GJ form which have the condition $|V_{cb}| = \sqrt{m_c/m_t}$ at the scale M_U , we also consider the equations

$$\frac{|V_{cb}|^2}{\left(\frac{m_c}{m_t}\right)} = \eta_c^{-1} e^{(-\frac{3}{2}b+3c)I_t + \frac{3}{2}cI_b} \quad (45)$$

$$= \eta_c^{-1} e^{-\frac{3}{2}I_t - \frac{3}{2}I_b} \quad (\text{SM}) \quad (46)$$

$$= \eta_c^{-1} e^{-\frac{1}{2}I_t + \frac{1}{2}I_b} \quad (2\text{HSM}) \quad (47)$$

$$= \eta_c^{-1} e^{-I_t + I_b} \quad (\text{MSSM}). \quad (48)$$

We see that, in all cases, the heavier the top quark is, the lower this ratio is. The first paper we know of that provides a renormalization group analysis of the relation $|V_{cb}| = \sqrt{m_c/m_t}$ is Ref. [28] which discusses the relation for the case of non-SUSY $SO(10)$ with an intermediate breaking scale M_I . We shall also discuss this relation in the context of non-SUSY $SO(10)$ in Secs. IV and V.

III. BRIEF REVIEW OF MSSM CASE (DHR ANSATZ)

In this section, we will look at the *Ansatz* of Dimopoulos, Hall, and Raby (DHR) [1] for the purpose of making the program we will use for the non-SUSY cases clear and also so that we may later compare results between the SUSY and non-SUSY cases. For a more complete analysis, see Refs. [1–3]. In the original DHR *Ansatz*, the the grand unification scale fermion Yukawa coupling matrices take the form

$$\mathbf{U} = \begin{pmatrix} 0 & C & 0 \\ C & 0 & B \\ 0 & B & A \end{pmatrix}, \quad \mathbf{D} = \begin{pmatrix} 0 & F & 0 \\ F & E & 0 \\ 0 & 0 & D \end{pmatrix}, \quad (49)$$

$$\mathbf{E} = \begin{pmatrix} 0 & F & 0 \\ F & -3E & 0 \\ 0 & 0 & D \end{pmatrix},$$

where A, B, C, D, E , and F are complex parameters, with

$$\begin{aligned} |A| &\gg |B| \gg |C|, \\ |D| &\gg |E| \gg |F|. \end{aligned} \quad (50)$$

(Note that the up quark mass matrix is of the Fritzsch form and that the down quark and charged lepton mass matrices implement the Georgi-Jarlskog mechanism.)

We recall that $\mathbf{M}_U = \mathbf{U}\kappa\sin\beta$, $\mathbf{M}_D = \mathbf{D}\kappa\cos\beta$, and $\mathbf{M}_E = \mathbf{E}\kappa\cos\beta$. After rotating away all but one unavoidable phase ϕ in the Yukawa coupling matrices by redefinition of the phases of the fermion fields [1], these matrices may be given the form

$$\mathbf{U} = \begin{pmatrix} 0 & C & 0 \\ C & 0 & B \\ 0 & B & A \end{pmatrix}, \quad \mathbf{D} = \begin{pmatrix} 0 & Fe^{i\phi} & 0 \\ Fe^{-i\phi} & E & 0 \\ 0 & 0 & D \end{pmatrix}, \quad (51)$$

$$\mathbf{E} = \begin{pmatrix} 0 & F & 0 \\ F & -3E & 0 \\ 0 & 0 & D \end{pmatrix},$$

where A, B, C, D, E , and F are now real. This *Ansatz* uses the eight inputs A, B, C, D, E, F, ϕ , and $\tan\beta$ to describe the SM fermion sector, which contains 13 independent parameters. Hence, these eight parameters may be fixed in terms of the eight best measured SM fermion sector parameters to yield five SM fermion sector predictions and $\tan\beta$ of the MSSM. The following inputs are used [29]:

$$m_b(m_b) = 4.25 \pm 0.1 \text{ GeV}, \quad (52)$$

$$m_\tau(m_\tau) = 1.784 \text{ GeV}, \quad (53)$$

$$m_c(m_c) = 1.27 \pm 0.05 \text{ GeV}, \quad (54)$$

$$m_\mu(m_\mu) = 105.658 \text{ MeV}, \quad (55)$$

$$0.2 \leq \frac{m_u(1 \text{ GeV})}{m_d(1 \text{ GeV})} \leq 0.7, \quad (56)$$

$$m_e(m_e) = 0.511 \text{ MeV}, \quad (57)$$

$$|V_{cb}| = 0.044 \pm 0.014, \quad (58)$$

$$|V_{us}| = 0.221 \pm 0.003. \quad (59)$$

The above masses are running masses in the $\overline{\text{MS}}$ scheme and their quoted uncertainties are at the 1σ level. For the CKM matrix parameters $|V_{cb}|$ and $|V_{us}|$, we have quoted the uncertainties at the 90% confidence level. The 1σ limit on $|V_{cb}|$ is $|V_{cb}| = 0.044 \pm 0.009$.

By finding the biunitary transformations that transform the mass matrices at the grand unification scale to diagonal matrices with real positive entries, making use of Eq. (50), and using the results of the RGE analysis of the previous section one may find the predictions [1] for the five SM parameters and $\tan\beta$ in terms of the previously given inputs. Four of these are the following:

$$\frac{m_d/m_s}{\left[1 - \frac{m_d}{m_s}\right]^2} = \frac{9 \frac{m_e}{m_\mu}}{\left[1 - \frac{m_d}{m_s}\right]^2}, \quad (60)$$

$$m_s - m_d = \frac{m_\mu \eta_s}{3 \eta_\mu} R_d^e, \quad (61)$$

$$\left| \frac{V_{ub}}{V_{cb}} \right| = \sqrt{\frac{3m_e \left(\frac{m_u}{m_d}\right) \eta_s \eta_c}{m_c \eta_u \eta_e} R_d^e}, \quad (62)$$

$$J = \sqrt{\frac{m_d}{m_s}} |V_{cb}|^2 \left| \frac{V_{ub}}{V_{cb}} \right| \sin\phi, \quad (63)$$

with

$$\cos\phi = \frac{|V_{us}|^2 - \left(\frac{m_d}{m_s}\right) - \left| \frac{V_{ub}}{V_{cb}} \right|^2}{2\sqrt{\frac{m_d}{m_s} \left| \frac{V_{ub}}{V_{cb}} \right|}}, \quad (64)$$

and where we have defined $R_d^e \equiv A_d/A_e$.

The fifth predicted SM parameter is m_t . An input value for $|V_{cb}|$ gives two possible pairs of predictions for m_t and the MSSM parameter $\tan\beta$. Only for the case that $\tan\beta$ is small can an accurate analytical approximation be given for m_t and $\tan\beta$. Otherwise, one must numerically integrate the RGE's. When $\tan\beta$ is assumed to be small, the following predictions can be made from the M_U scale conditions $|V_{cb}| = \sqrt{m_c/m_t}$ and $m_b = m_\tau$ with the RGE's given in the last section:

$$m_t(m_t) = \frac{m_c/\eta_c}{|V_{cb}|^2} \frac{b}{\tau}, \quad (65)$$

$$\sin\beta = \frac{\sqrt{K_u} m_c/\eta_c}{A_u \kappa |V_{cb}|^2} \left(\frac{\tau}{b}\right)^5 \left[\left(\frac{\tau}{b}\right)^{12} - 1 \right]^{-\frac{1}{2}}, \quad (66)$$

and, for the unification scale top quark Yukawa coupling,

$$A = K_u^{-\frac{1}{2}} \sqrt{\left(\frac{\tau}{b}\right)^{12} - 1}, \quad (67)$$

where we have again used the definitions

$$\tau \equiv \frac{m_\tau}{\eta_\tau A_e}, \quad (68)$$

$$b \equiv \frac{m_b}{\eta_b A_d}, \quad (69)$$

and m_t is the running mass. As is well known, the $\overline{\text{MS}}$ scheme running mass is related to the physical pole mass by the relation

$$m_t^{\text{pole}} = m_t \left(1 + \frac{4\alpha_3(m_t)}{3\pi} + O(\alpha_3^2(m_t)) \right). \quad (70)$$

Now, we need to know what ranges of values are acceptable for the output parameters. For the purpose of comparing later with the non-SUSY cases, we will give the results for the previously mentioned example of $M_S = 180 \text{ GeV}$ and $\alpha_{3c}(M_Z) = 0.121$. For this value of $\alpha_3(M_Z)$, we find $\alpha_3(\mu_t) = 0.110$ and the following η_i 's:

$$\eta_b = 1.56, \quad (71)$$

$$\eta_c = 2.19, \quad (72)$$

$$\eta_s = 2.54, \quad (73)$$

$$\eta_u = 2.55. \quad (74)$$

For the outputs m_s/m_d and m_s , acceptable ranges are [29]

$$15 \leq \frac{m_s(1 \text{ GeV})}{m_d(1 \text{ GeV})} \leq 25, \quad (75)$$

$$m_s(1 \text{ GeV}) = 175 \pm 55 \text{ MeV}. \quad (76)$$

In Ref. [29], larger values of m_s/m_d correspond to smaller values of m_u/m_d . Determined solely by the ratio m_e/m_μ , the prediction for m_s/m_d is

$$\frac{m_s}{m_d} = 24.71, \quad (77)$$

which is at the upper end of its acceptable range. (Of course, this ratio does not depend on whether the case considered is supersymmetric.) The prediction for m_s is 206 GeV.

The 1σ experimental limits on the CKM parameter $|V_{ub}/V_{cb}|$ are

$$\left| \frac{V_{ub}}{V_{cb}} \right| = 0.09 \pm 0.04. \quad (78)$$

For our example, the prediction is $|V_{ub}/V_{cb}| = 0.059 \sqrt{\frac{m_u}{m_d} \frac{1.27 \text{ GeV}}{m_c}}$. The possible range for $|V_{ub}/V_{cb}|$ is shown in Fig. 1(a). For this typical example, we can see that $|V_{ub}/V_{cb}|$ varies from the lower end of accept-

ability 0.05 up to about 0.0665.

For the CP -violating parameter J , we find $J \times 10^5 = 2.9 \left(\frac{|V_{cb}|}{0.05} \right)^2$ when $m_u/m_d = 0.6$ and $m_c = 1.27 \text{ GeV}$. In Fig. 1(b) for the case of $m_u/m_d = 0.6$ and $m_c = 1.27 \text{ GeV}$, we plot J as a function of $|V_{cb}|$ for values of $|V_{cb}|$ less than 0.053 and greater than 0.044, which is the allowed range of $|V_{cb}|$ within its 1σ experimental limits. The plot shows that under these conditions $J \times 10^5$ can range from 2.2 to 3.3. In Fig. 2, we also plot $\cos \phi$ as a function of $|V_{ub}/V_{cb}|$ over its predicted range. This plot is of course also applicable to the non-SUSY cases to be discussed. The range of $\cos \phi$ shown is from 0.14 to 0.30. The significance of $\cos \phi$ for experiment is given in Ref. [30].

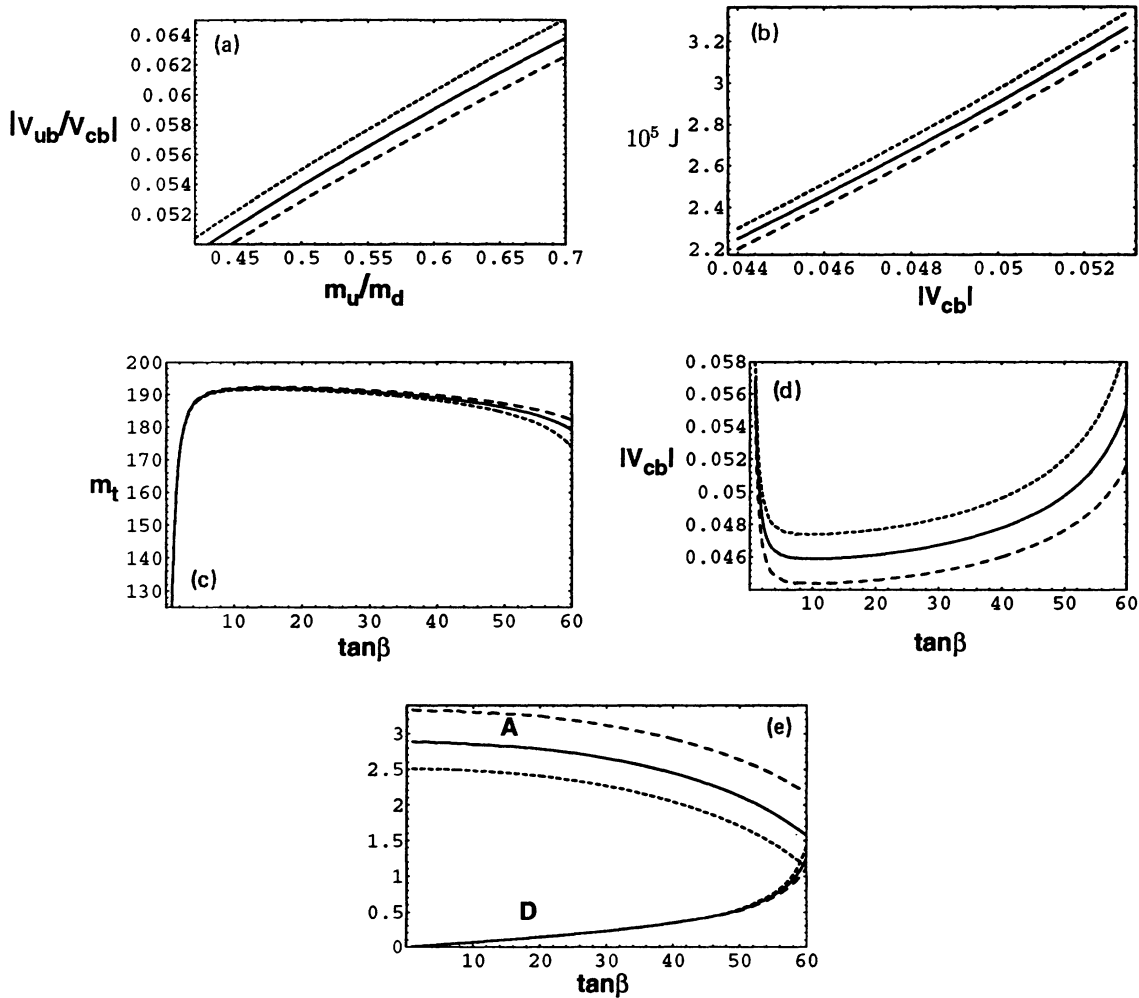


FIG. 1. In this figure, we show the following results for the MSSM example discussed in Sec. III. (a) The prediction for $|V_{ub}/V_{cb}|$ vs input values of m_u/m_d . The short-dashed line, solid line, and the long-dashed line represent the cases where m_c is 1.22 GeV, 1.27 GeV, and 1.32 GeV, respectively. (b) The prediction for the CP violation parameter J vs input values of $|V_{cb}|$. The short-dashed line, solid line, and the long-dashed line represent the cases where m_c is 1.22 GeV, 1.27 GeV, and 1.32 GeV, respectively. (c) The prediction for the running mass m_t as a function of $\tan \beta$ for $m_t > 125 \text{ GeV}$ and $\tan \beta \leq 60$. The short-dashed line, solid line, and the long-dashed line represent the cases where m_b is 4.35 GeV, 4.25 GeV, and 4.15 GeV, respectively. (d) The CKM matrix parameter $|V_{cb}|$ as a function of $\tan \beta$. The short-dashed line, the solid line, and the long-dashed line represent the same values of m_b as in (c) and also the values 1.32 GeV, 1.27 GeV, and 1.22 GeV for m_c , respectively. (e): The M_U scale top and bottom Yukawa couplings as a function of $\tan \beta$. The short-dashed line, the solid line, and the long-dashed line represent the same values of m_b as in (c).

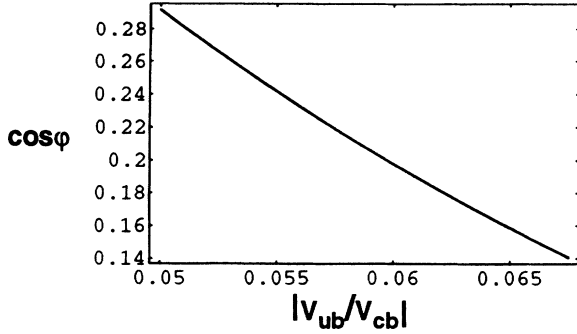


FIG. 2. The cosine of the complex phase that appears in the DHR *Ansätze* as a function of the input $|V_{ub}/V_{cb}|$.

Next, we look at the predictions made for m_t and $\tan\beta$. In Refs. [2, 3], it was determined that each value of m_t has two values of $\tan\beta$ associated with it. Since each value of $\tan\beta$ has only one value of m_t and one value of $|V_{cb}|$ associated with it, in Fig. 1(c) we plot m_t vs $\tan\beta$ and in Fig. 1(d) we plot $|V_{cb}|$ vs $\tan\beta$. Here, we plot the region described by $\tan\beta \leq 60$ and $m_t \geq 125$ GeV. As in Refs. [2, 3], for each value of $\tan\beta$ we numerically integrate the RGE's from the scale $\mu_t = 180$ GeV for different values of m_t until we find one that gives $\lambda_{b\nu}$ and $\lambda_{\tau\nu}$ to be within 0.1% of each other at the grand unification scale M_U . From recent direct top searches, $m_t^{\text{pole}} \geq 131$ GeV [31]. According to the analysis of the most recent electroweak data [26], $m_t^{\text{pole}} \leq 180$ GeV. The figure shows that the top mass is within these bounds only for some values of small $\tan\beta$ and for large $\tan\beta \sim 60$.

As in Ref. [3], we also plot in Fig. 1(e) the grand unification scale couplings A and D as a function of $\tan\beta$. At about $\tan\beta = 58$, we can see that $D = A$ for the example $m_b = 4.35$ GeV. (For both of the other two examples graphed, $D = A$ for some $\tan\beta$ a little greater than 60.) In Refs. [2, 3] it was shown that one may use the unification scale condition $D = A$ to decrease by 1 the number of inputs in the *Ansatz* and hence increase its number of predictions to five SM parameters and $\tan\beta$. With $D = A$ at M_U , $|V_{cb}|$ [2, 3] can now also be predicted.

Finally, we review work done on the neutrino sector and the possibility of there being an *Ansatz* to predict the neutrino masses and the leptonic mixing angles. In Ref. [32], DHR propose the following *Ansätze* for the neutrino Dirac mass matrix and Majorana mass matrix, respectively:

$$M_{\nu N} = \begin{pmatrix} 0 & -3C & 0 \\ -3C & 0 & -3\kappa B \\ 0 & -3\kappa B & -3A \end{pmatrix} \kappa \sin\beta \quad (79)$$

and

$$M_{NN} = \begin{pmatrix} 0 & C & 0 \\ C & 0 & 0 \\ 0 & 0 & A \end{pmatrix} V, \quad (80)$$

where V is the superheavy singlet VEV and $\kappa = 1$ or $-1/3$. The low mass neutrino mass matrix is then of the form

$$M_{\nu\nu} = M_{\nu N} M_{NN}^{-1} M_{\nu N}^T. \quad (81)$$

Then, just as in the quark sector, from bilinear transformations $M_E^{\text{diag}} = V_e^L M_E V_e^{R\dagger}$ and $M_{\nu\nu}^{\text{diag}} = V_\nu^L M_{\nu\nu} V_\nu^{R\dagger}$ that diagonalize the lepton mass matrices one finds the leptonic CKM matrix $V' = V_\nu V_e^{L\dagger}$. DHR then find the following neutrino mass ratios and mixing angles:

$$\frac{m_{\nu\tau}}{m_{\nu\mu}} = \frac{1}{3\kappa^2} \left(\frac{B}{A}\right)^{-2}, \quad (82)$$

$$\frac{m_{\nu\mu}}{m_{\nu e}} = 9\kappa^4 \frac{m_c \eta_u}{m_u \eta_c}, \quad (83)$$

$$\theta_{\mu\tau} \simeq -2\kappa \frac{B}{A}, \quad (84)$$

$$\theta_{e\mu} \simeq \left[\frac{m_e}{m_\mu} + \frac{m_{\nu e}}{m_{\nu\mu}} - 2\sqrt{\frac{m_e m_{\nu e}}{m_\mu m_{\nu\mu}}} \cos\phi \right]^{\frac{1}{2}}, \quad (85)$$

$$\theta_{e\tau} \simeq \frac{2}{3}\kappa \sqrt{\frac{m_e}{m_\mu}} \frac{B}{A}, \quad (86)$$

in which $B/A = |V_{cb}(M_U)|$.

For our example with $\kappa = 1$ and assuming $\tan\beta$ to be small, we find

$$\frac{m_{\nu\tau}}{m_{\nu\mu}} = 278, \quad (87)$$

$$\frac{m_{\nu\mu}}{m_{\nu e}} = 3680, \quad (88)$$

$$\sin^2 \theta_{\mu\tau} = 0.0191, \quad (89)$$

$$\sin^2 \theta_{e\mu} = 0.0177, \quad (90)$$

$$\sin^2 \theta_{e\tau} = 1.03 \times 10^{-5}, \quad (91)$$

where we have used $|V_{cb}| = 0.05$, $m_u/m_d = 0.43$, and $m_c = 1.23$ GeV. We used $m_u/m_d = 0.43$ and $m_c = 1.23$ GeV to get $\sin^2 \theta_{e\mu}$ as low as possible. The value of $\sin^2 \theta_{e\mu}$ and the mass ratios found in this example are to be compared with the small mixing-angle nonadiabatic solution window [$\Delta m^2 \simeq (0.3-1.2) \times 10^{-5}$ eV² and $\sin^2 \theta_{e\mu} \simeq (0.4-1.5) \times 10^{-2}$] which is in agreement with all experimental data [33]. The value of $m_{\nu\tau}$ is ~ 1 eV. The $\kappa = -1/3$ scenario can only provide neutrino masses and mixing that lie well between the small and large angle 90% confidence limit Mikheyev-Smirnov-Wolfenstein (MSW) solution windows [32].

IV. ANSATZ IN THE SM

As discussed in Sec. II, the unification of m_b and m_τ at an intermediate symmetry-breaking scale M_I is not possible in the SM cases. Wanting both to have an acceptable value of m_b and use mass matrices as similar as possible to the GJ form, we will use the following *Ansatz* at M_U :

$$\mathbf{U} \sim \begin{pmatrix} 0 & C & 0 \\ C & 0 & B \\ 0 & B & A \end{pmatrix}, \quad \mathbf{D} \sim \begin{pmatrix} 0 & F & 0 \\ F & E & 0 \\ 0 & 0 & D+d \end{pmatrix}, \quad \mathbf{E} \sim \begin{pmatrix} 0 & F & 0 \\ F & -3E & 0 \\ 0 & 0 & D-3d \end{pmatrix}, \quad (92)$$

where $A, B, C, D, d, E,$ and F are complex parameters, with $|A| \gg |B| \gg |C|$ and $|D + d| \sim |D - 3d| \gg |E| \gg |F|$.

Below the grand unification scale, the zero entries in the mass matrices will develop small finite values. However, we have found the values that these entries develop when one takes the energy scale from the grand unification scale down to the intermediate breaking scale are negligible. So, it is a good approximation to take the *Ansatz* at the intermediate breaking scale. (Most importantly, $|V_{cb}|/\sqrt{\frac{m_c}{m_t}}$ does not evolve between M_U and M_I .) After rotating away all but one unavoidable phase ϕ in the mass matrices by redefinition of the phases of the fermion fields [1], we take the *Ansatz* at the intermediate breaking scale to be

$$\mathbf{U} \sim \begin{pmatrix} 0 & C & 0 \\ C & 0 & B \\ 0 & B & A \end{pmatrix}, \mathbf{D} \sim \begin{pmatrix} 0 & F e^{i\phi} & 0 \\ F e^{-i\phi} & E & 0 \\ 0 & 0 & |D + d| \end{pmatrix}, \mathbf{E} \sim \begin{pmatrix} 0 & F & 0 \\ F & -3E & 0 \\ 0 & 0 & |D - 3d| \end{pmatrix}. \quad (93)$$

Although this *Ansatz* lacks bottom- τ Yukawa coupling unification, it uses the same number, 3, of parameters to describe the third-generation masses as does the MSSM or 2HSM cases with bottom- τ Yukawa coupling unification because they require the additional parameter $\tan\beta = \kappa_u/\kappa_d$. D and d may always be chosen to satisfy experimentally determined values of m_b and m_τ , but do not make predictions. Besides the two parameters D and d our *Ansatz* has six other parameters, and other than m_b and m_τ the SM has eleven fermion sector parameters. So we can make five predictions from the six of these eleven fermion sector parameters that are best determined. We use $m_e, m_\mu, m_c, m_u/m_d, |V_{cb}|,$ and $|V_{ub}|$ as inputs. In the last section, we quoted acceptable values for these parameters.

Now we look at the predictions for $m_t, m_s, m_s/m_d, |V_{ub}/V_{cb}|,$ and the CP violation parameter J (or $\cos\phi$). Note that these are the same SM quantities as predicted for the DHR model without top-bottom Yukawa coupling unification. (The DHR model predicts these five SM parameters and also the SUSY parameter $\tan\beta = \kappa_u/\kappa_d$.) We will look at predictions for two cases. For case (a) we use $M_I = 10^{10.94}$ GeV, and for case (b) we use $M_I = 10^{14}$ GeV.

First, from Eqs. (19), (22), (26), and (32),

$$m_t = \frac{m_c/\eta_c}{\sqrt{|V_{cb}|^4 + \frac{K_u}{\kappa^2 A_u^2} \left(\frac{m_c}{\eta_c}\right)^2}}. \quad (94)$$

We show running mass m_t vs $|V_{cb}|$ for the SM scenario in Fig. 3(a) for case (a) and in Fig. 4(a) for case (b). In case (a) we see that $|V_{cb}|$ can be as low as 0.039, and in case (b) $|V_{cb}|$ can be as low as 0.038 for running mass m_t less than 200 GeV. For $|V_{cb}|$ within its 1σ limits, in case (a) m_t can be as low as about 140 GeV and in case (b) m_t can be as low as 145 GeV.

Now we look at the other four predictions. These four predictions all take the same form as in the original DHR *Ansatz* and are given by Eq. (60), Eq. (61), Eq. (62), and Eq. (63). Of course, the prediction for m_s/m_d is the same as before $m_s/m_d = 24.71$ because it only depends on the ratio m_e/m_μ . The other three predictions are proportional to the ratio of the gauge contribution for the down quark masses to the gauge contribution for the charged lepton masses $R_d = A_d/A_e$.

Since the prediction for m_s is proportional to R_d , the range of predicted values of m_s in the SM case (a) has

to be lower than the range of predicted value in the SM case (b). In case (a) we find

$$m_s = 160_{-23}^{+40} \text{ MeV}, \quad (95)$$

and in case (b) we find

$$m_s = 177_{-25}^{+55} \text{ MeV}. \quad (96)$$

The uncertainties that we give are due to the uncertainty in $\alpha_3(M_Z)$. The value in our MSSM example was $m_s = 191$ GeV, which is contained in the upper part of the range of values for the SM case (a).

Also, the prediction for $|V_{ub}^k|$ is proportional to R_d . So, once again, we expect the range of predicted values for $|V_{ub}^k|$ in the SM case (a) to be lower than the range of predicted values in the SM case (b). In the SM case (a) we find

$$\left| \frac{V_{ub}}{V_{cb}} \right| = (0.053_{-0.003}^{+0.004}) \sqrt{\frac{m_u}{m_d} \frac{1.27 \text{ GeV}}{m_c}}, \quad (97)$$

and in the SM case (b) we find

$$\left| \frac{V_{ub}}{V_{cb}} \right| = (0.055_{-0.003}^{+0.005}) \sqrt{\frac{m_u}{m_d} \frac{1.27 \text{ GeV}}{m_c}}. \quad (98)$$

The uncertainties given here are due to the uncertainty in $\alpha_3(M_Z)$. The value in our MSSM example was $\left| \frac{V_{ub}^k}{V_{cb}} \right| = 0.059 \sqrt{\frac{m_u}{m_d} \frac{1.27 \text{ GeV}}{m_c}}$, which is contained in the upper part of the range of values for the SM case (a). We show the range of good values for $|V_{ub}/V_{cb}|$ in Fig. 3(b) for the SM case (a) and in Fig. 4(b) for the SM case (b).

Being proportional to R_d , one expects the CP violation parameter J to have a lower range of predicted values in the SM case (a) than in the SM case (b). When $m_u/m_d = 0.6$ and $m_c = 1.27$ GeV, we find

$$J \times 10^5 = (2.6_{-0.2}^{+0.3}) \left(\frac{|V_{cb}|}{0.05} \right)^2 \quad (99)$$

for the SM case (a) and

$$J \times 10^5 = (2.7 \pm 0.2) \left(\frac{|V_{cb}|}{0.05} \right)^2 \quad (100)$$

for the SM case (b). This is to be compared with $J \times 10^5 = 2.9 \left(\frac{|V_{cb}|}{0.05} \right)^2$ in the MSSM case. The prediction for

case (a) is plotted in Fig. 3(c), and the prediction for case (b) is plotted in Fig. 4(c). The predicted values for $\cos \phi$ can again be found from Fig. 2 for the predicted ranges of $|V_{ub}/V_{cb}|$.

To complete this section, we will consider neutrino

mass matrices of the form given in Eq. (79) and Eq. (80). However, as a good approximation we will take the matrices at M_I instead of M_U . Following the same analysis as discussed in the last section, we find the following for case (a) when $|V_{cb}| = 0.05$, $m_u/m_d = 0.51$, $m_c = 1.27$ GeV, and $\alpha_{3c}(M_Z) = 0.118$:

$$\frac{m_{\nu\tau}}{m_{\nu\mu}} = 109, \tag{101}$$

$$\frac{m_{\nu\mu}}{m_{\nu e}} = 3720, \tag{102}$$

$$\sin^2 \theta_{\mu\tau} = 0.0483, \tag{103}$$

$$\sin^2 \theta_{e\mu} = 0.0176, \tag{104}$$

$$\sin^2 \theta_{e\tau} = 2.64 \times 10^{-5}, \tag{105}$$

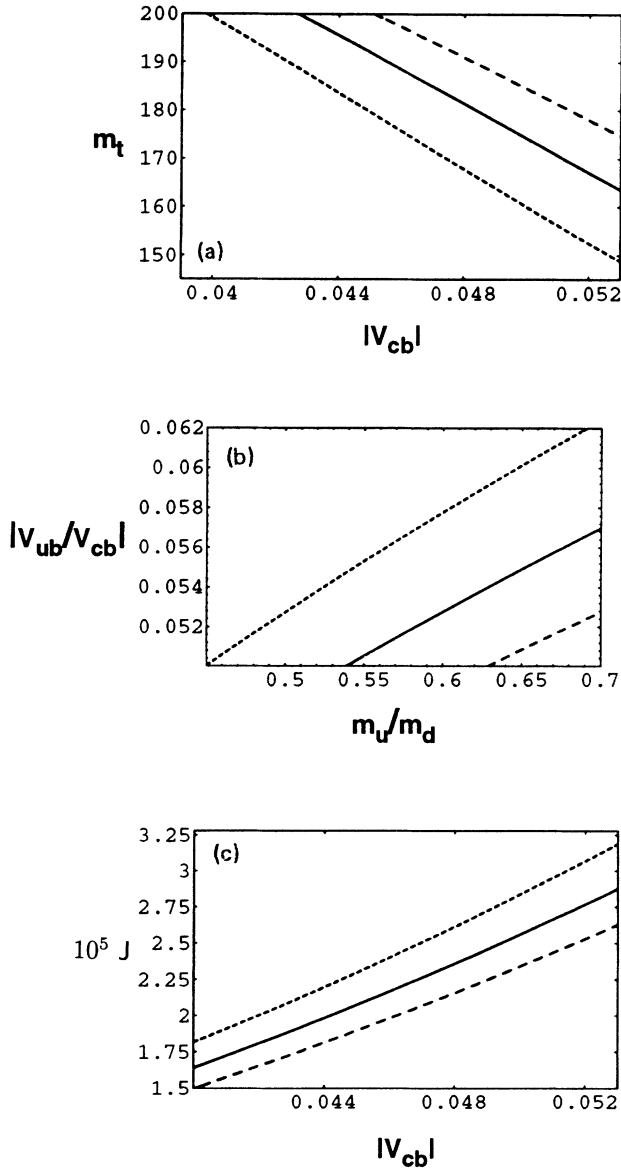


FIG. 3. In this figure we show the following predictions for the SM case (a) with $M_I = 10^{10.93}$ GeV discussed in Sec. IV. (a) The prediction for the running mass m_t vs $|V_{cb}|$. The short-dashed line represents the case where $m_c = 1.22$ GeV and $\alpha_{3c}(M_Z) = 0.125$. The solid line represents the case where $m_c = 1.27$ GeV and $\alpha_{3c}(M_Z) = 0.118$. The long-dashed line represents the case where $m_c = 1.32$ GeV and $\alpha_{3c}(M_Z) = 0.111$. (b) The prediction for $|V_{ub}/V_{cb}|$ vs input values of m_u/m_d . The short-dashed line, the solid line, and the long-dashed line represent the same values of m_c and $\alpha_{3c}(M_Z)$ as in (a). (c) The prediction for the CP violation parameter J vs input values of $|V_{cb}|$. The short-dashed line, the solid line, and the long-dashed line represent the same values of m_c and $\alpha_{3c}(M_Z)$ as in (a).

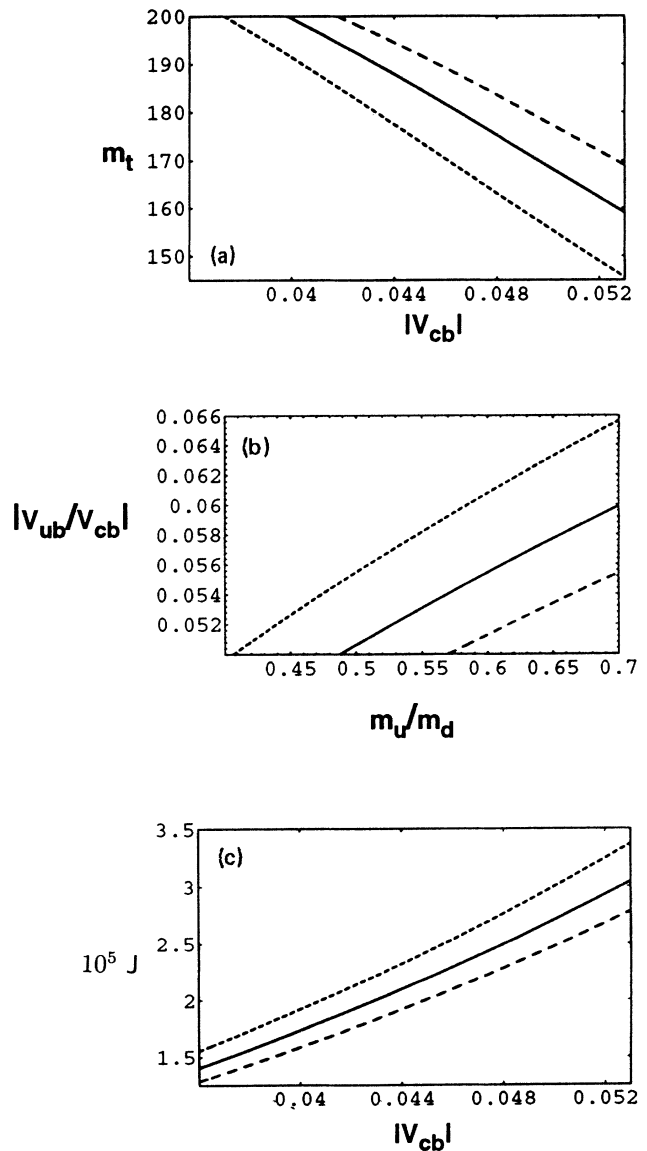


FIG. 4. In this figure we show some predictions for the SM case (b) with $M_I = 10^{14}$ GeV discussed in Section IV. (a), (b), and (c) are described by the captions for Figs. 3(a), 3(b), and 3(c), respectively.

and we find the following for case (b) when $|V_{cb}| = 0.05$, $m_u/m_d = 0.46$, $m_c = 1.27$ GeV, and $\alpha_{3c}(M_Z) = 0.118$:

$$\frac{m_{\nu_\tau}}{m_{\nu_\mu}} = 106, \quad (106)$$

$$\frac{m_{\nu_\mu}}{m_{\nu_e}} = 3730, \quad (107)$$

$$\sin^2 \theta_{\mu\tau} = 0.0493, \quad (108)$$

$$\sin^2 \theta_{e\mu} = 0.0176, \quad (109)$$

$$\sin^2 \theta_{e\tau} = 2.69 \times 10^{-5}. \quad (110)$$

Because $|V_{cb}|$ becomes larger at higher energies in the SM whereas it becomes smaller at higher energies in the MSSM, the values for $\sin^2 \theta_{e\mu}$ are virtually the same in the MSSM and SM cases whereas the ratio m_{ν_τ}/m_{ν_μ} is more than twice as big in the MSSM example than in the SM cases. The value of m_{ν_τ} is $\sim \frac{1}{2}$ eV.

V. ANSATZ IN THE 2HSM

For the 2HSM case, we first use an *Ansatz* of the form given in Eq. (49) at the grand unification scale. Although the zero entries in the Yukawa matrices will develop relatively small values between M_U and M_I , $|V_{cb}|/\sqrt{\frac{m_c}{m_t}}$ does not evolve over that range and so as a good approximation one can effectively take the *Ansatz* at M_I in the form of Eq. (51). Like the DHR *Ansatz*, this *Ansatz* has eight parameters. So it is possible to predict five SM fermion sector parameters and the 2HSM parameter $\tan \beta$ in terms of the eight best measured SM fermion sector parameters. Of course, we choose the same five input parameters as in Sec. III. The expressions for the four output parameters m_s , m_s/m_d , $|V_{ub}/V_{cb}|$, and the *CP* violation parameter J (or $\cos \phi$) again are given by Eq. (60), Eq. (61), Eq. (62), and Eq. (63). Since in the 2HSM $R_d = A_d/A_e$ has values within a few percent of its values in the SM case (a), these four 2HSM case predictions will only be slightly different than the predictions of these 4 parameters that were given for the SM case (a). Those predictions are already given in Table II and Fig. 3. However, we do need to discuss the predictions for m_t and $\tan \beta$.

If we are to require $\lambda_{b_U} = \lambda_{\tau_U}$ but not $\lambda_{t_U} = \lambda_{\tau_U}$, then

we must have two Higgs bidoublets instead of one in the intermediate scale effective theory. (Hence for this case the model needs two complex **10**'s instead of the minimal one complex **10**.) One Higgs doublet from each of these bidoublets is then assumed to contain a VEV and appear in the 2HSM effective theory below M_I . (One Higgs doublet is ϕ_u and the other is ϕ_d .) For the more interesting case of $\lambda_{t_U} = \lambda_{b_U} = \lambda_{\tau_U}$, the model only needs one Higgs bidoublet appearing at intermediate scales, and hence the model only needs the minimal one complex **10** Higgs field. The A_α 's and the K_u 's which we give in Table I for the 2HSM case and use in this section were calculated for the assumption of only one Higgs bidoublet having a mass less than M_U . The M_I we use is calculated according to the survival hypothesis and $\alpha_{3c}(M_Z) = 0.018$. The values of the A_α 's and the K_u 's that are calculated for the two-Higgs-bidoublet case are similar to the corresponding values given for the single-Higgs-bidoublet case, and one would expect these differences to be smaller than the uncertainties in the A_α 's and the K_u 's due to possible threshold corrections which we ignore for the sake of simplicity.

When the assumption of $\tan \beta$ being small is made, m_t and $\tan \beta$ may be predicted to a very good approximation by the equations

$$m_t(m_t) = \frac{m_c/\eta_c}{|V_{cb}|^2} \frac{b}{\tau}, \quad (111)$$

$$\sin \beta = \frac{\sqrt{K_u} m_c/\eta_c}{A_u \kappa |V_{cb}|^2} \left(\frac{\tau}{b}\right)^8 \left[\left(\frac{\tau}{b}\right)^{18} - 1\right]^{-\frac{1}{2}}, \quad (112)$$

and for the intermediate breaking scale top quark Yukawa coupling,

$$A = K_u^{-\frac{1}{2}} \sqrt{\left(\frac{\tau}{b}\right)^{18} - 1}, \quad (113)$$

where we have again used $\tau = m_\tau/\eta_\tau A_e$ and $b = m_b/\eta_b A_d$, and m_t is the top quark running mass. In order to investigate the situation for when $\tan \beta$ is not small we must numerically integrate the Yukawa RGE's to find for each value of $\tan \beta$ a value of m_t for which λ_{b_I} agrees with λ_{τ_I} to within 0.1%.

We have found two separate ranges of $\tan \beta$ that give values for the running mass m_t between 125 GeV and

TABLE II. This table lists three of the five SM predictions made by SM case (a) ($M_I = 10^{10.94}$ GeV) and SM case (b) ($M_I = 10^{14}$ GeV) and those same three parameters as predicted by the DHR *Ansatz* with $M_S = 180$ GeV and $\alpha_3(M_Z) = 0.121$. M_I is the scale at which the intermediate gauge symmetry $\{2_L 2_R 4_C\}$ breaks to the SM.

Parameter	Prediction for SM case (a)	Prediction for SM case (b)	Prediction for MSSM
$m_s(1 \text{ GeV})$	$160_{-23}^{+40} \text{ MeV}$	$177_{-25}^{+55} \text{ MeV}$	206 MeV
$ V_{ub}/V_{cb} $	$(0.053_{-0.003}^{+0.004}) \sqrt{\frac{m_u}{m_d} \frac{1.27 \text{ GeV}}{m_c}}$	$(0.055_{-0.003}^{+0.005}) \sqrt{\frac{m_u}{m_d} \frac{1.27 \text{ GeV}}{m_c}}$	$0.059 \sqrt{\frac{m_u}{m_d} \frac{1.27 \text{ GeV}}{m_c}}$
$J \cdot 10^5$	$(2.6 \pm 0.2) \left(\frac{ V_{cb} }{0.05}\right)^2$	$(2.7 \pm 0.2) \left(\frac{ V_{cb} }{0.05}\right)^2$	$2.9 \left(\frac{ V_{cb} }{0.05}\right)^2$
for $\frac{m_u}{m_d} = 0.6$ and $m_c = 1.27 \text{ GeV}$			

200 GeV. One region is for $\tan\beta \sim 1$ and has A much greater than D . In the other region, $\tan\beta$ is greater than about 55 and D is of the same order as or larger than A . It is not surprising that we find two separate regions in $\tan\beta$. One expects the m_t vs $\tan\beta$ plot for the 2HSM case to have the same shape as the m_t vs $\tan\beta$ plot for the MSSM case in Fig. 1(c), but one also expects as discussed in Sec. II that in both cases when A is much larger than D and $\sin\beta \approx 1$ the top mass required by the M_I scale condition $m_b = m_\tau$ will be close to $\kappa A_u / \sqrt{K_u}$. While $\kappa A_u / \sqrt{K_u}$ is a little smaller than 200 GeV in the MSSM case, it is larger than 200 GeV in the 2HSM case. Hence, one would expect m_t to be unacceptably large for intermediate values of $\tan\beta$ for which $\sin\beta \approx 1$ and A is much larger than D .

For the case that $\alpha_3(M_Z) = 0.111$ and $m_c = 1.22$ GeV, we find that for a small span of $\tan\beta$ (~ 1) from about 0.6 to about 1.7 the running mass m_t takes values from 125 GeV to 200 GeV. Within this region, $|V_{cb}|$ could be as low as about 0.053. When m_b has the values 4.35 GeV, 4.25 GeV, and 4.15 GeV, the M_I scale coupling $A = \lambda_{t_i}$ has the values 1.4, 1.8, and 2.3, respectively. (Larger input values for m_b give smaller values for A .) However, from Eq. (35) we find that $A = \lambda_{t_i}$ can have a maximum value of 1.26. The effect of using larger values of $\alpha_3(M_Z)$ is to require larger values of A than just given for the $\alpha_3(M_Z) = 0.111$ case (e.g., when $m_b = 4.35$ GeV and $\alpha_3(M_Z) = 0.118$, A must be 2.3). This lower region is ruled out in the scheme we are using unless the running mass m_b is larger than about 4.4 GeV and $\alpha_{3c}(M_Z)$ is near its lower end of acceptability.

In Fig. 5(a) and Fig. 5(b), we show the running mass m_t vs $\tan\beta$ and $|V_{cb}|$ vs $\tan\beta$ respectively for the higher region of $\tan\beta$ for the case that $\alpha_3(M_Z) = 0.111$ and $m_c = 1.22$ GeV. In the m_t vs $\tan\beta$ plot, we plot m_t for values of M_I scale Yukawa couplings A and D less than 1.3. We see that for $m_b = 4.35$ GeV, m_t can be as low as 150 GeV. In the $|V_{cb}|$ vs $\tan\beta$ plot, we can see that $|V_{cb}|$ is never within the 1σ limits of $|V_{cb}|$ but can be within its 90% confidence limits. In Fig. 5(c), we also show the unification scale couplings A and D as a function of $\tan\beta$. We can see that for the case with $m_b = 4.35$ GeV top-bottom- τ unification ($D = A$) is possible for $A \approx 0.8$.

In Figs. 6(a)–6(d), we show m_b , m_t , $|V_{cb}|$, and $\tan\beta$ as a function of A when $D = A$ for the case where $\alpha_3(M_Z) = 0.111$ and $m_c = 1.22$ GeV. Using a value of m_b as an input determines a value for A , but only values of m_b more than 4.25 GeV predict values of m_t less than 200 GeV. In fact, for $m_b \leq 4.4$ GeV the top running mass is predicted to be high, greater than 180 GeV. Once again, the possible range for $|V_{cb}|$ lies outside of its 1σ limits but within its 90% confidence limits. The value for $\tan\beta$ is predicted to be between 57.5 and 65 for $m_t < 200$ GeV. The M_I scale Yukawa coupling A takes values from 0.73 to 1.00 for $m_b \leq 4.4$ GeV.

Figures 6(a)–6(d) for the 2HSM case can be compared with the situation in the MSSM. In Figs. 7(a)–7(d), we show m_b , m_t , $|V_{cb}|$, and $\tan\beta$ as a function of A when $D = A$ for the case when $\alpha_3(M_Z) = 0.121$, $M_S = 180$ GeV, and $m_c = 1.22$ GeV. We see that in the MSSM,

having m_b within the 90% limits given in Ref. [29], corresponds to lower values of m_t than in the 2HSM case just discussed. For example, $m_b = 4.4$ GeV corresponds to a running mass $m_t = 174.5$ GeV, which is a pole mass of 183 GeV. Although its values are found to be lower than in the 2HSM, $|V_{cb}|$ comes out just above its 1σ limits. As in the 2HSM case, $\tan\beta \sim 60$.

Bottom τ Yukawa coupling unification in the 2HSM with $\alpha_3(M_Z) = 0.118$ requires high values of m_b to keep

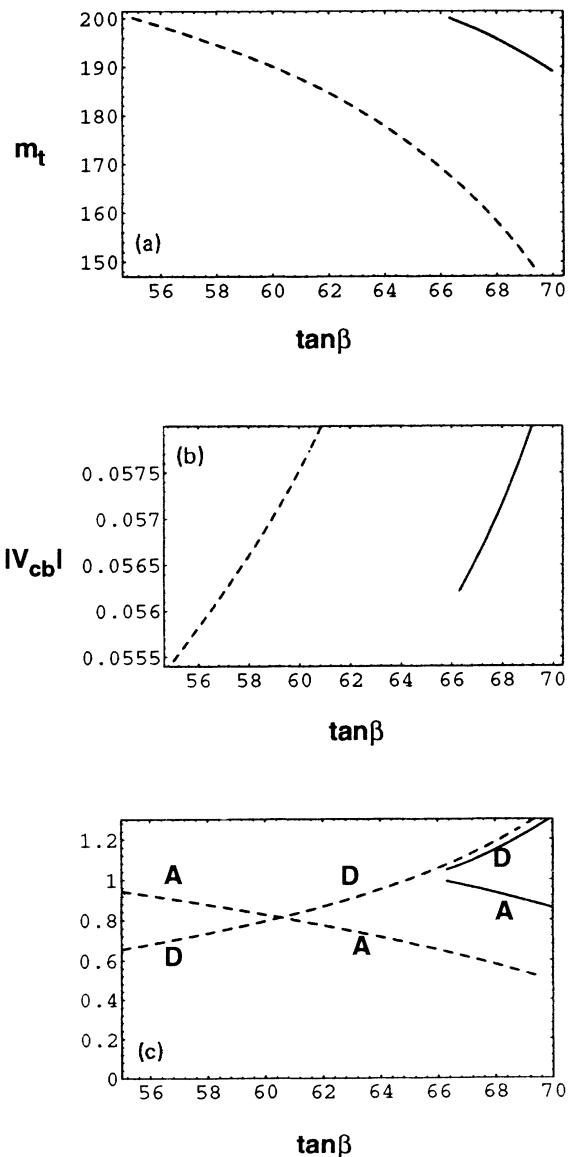


FIG. 5. In this figure we show the following predictions for the 2HSM case with $M_I = 10^{11.28}$ GeV discussed in Sec. IV. (a) The running mass m_t vs $\tan\beta$ with the dashed line and the solid line representing $m_b = 4.35$ GeV and $m_b = 4.25$ GeV, respectively. We show m_t between 125 GeV and 200 GeV. (b) The CKM parameter $|V_{cb}|$ as a function of $\tan\beta$ with $m_c = 1.22$ GeV and the dashed and solid line representing the same as in (a) (c): The M_I scale top and bottom Yukawa couplings A and D plotted as a function of $\tan\beta$ with the dashed and solid lines representing the same as in (a).

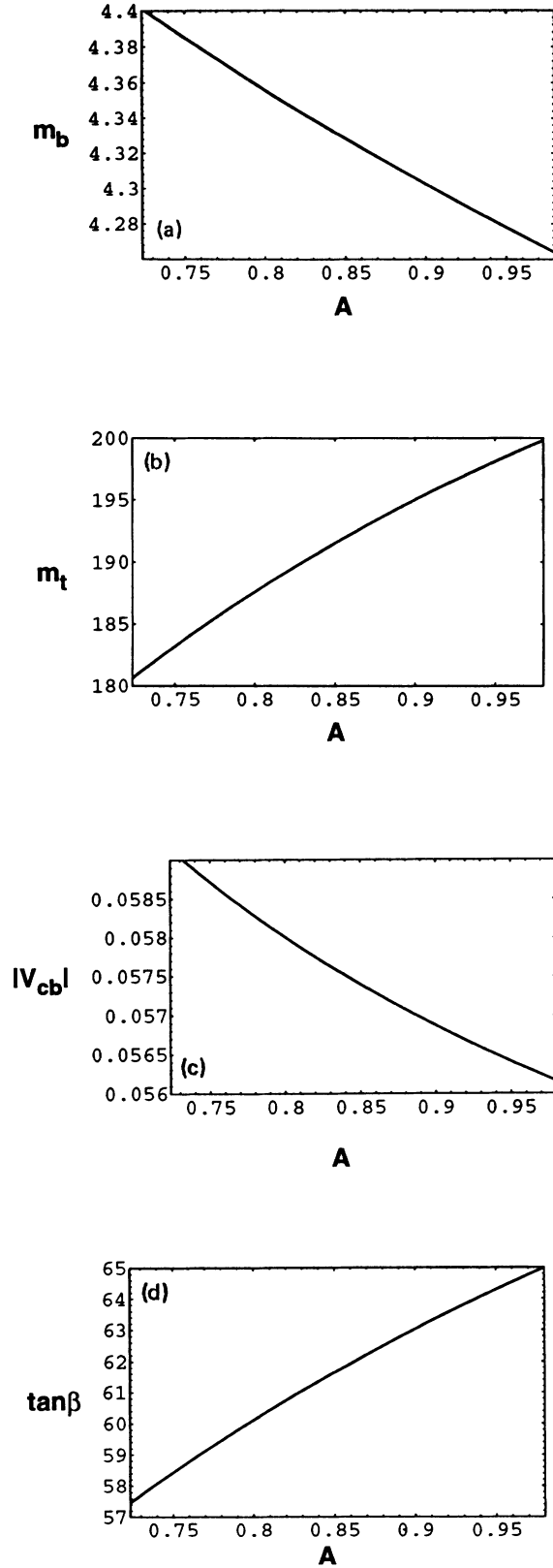


FIG. 6. For the case of $A \equiv \lambda_{t_I} = \lambda_{b_I} = \lambda_{\tau_I}$ in the 2HSM case of Sec. V with $M_I = 10^{11.28}$ GeV, we plot running mass m_b , running mass m_t , $|V_{cb}|$, and $\tan\beta$ as a function of A in (a), (b), (c), and (d), respectively. In (c), we use $m_c = 1.22$ GeV.

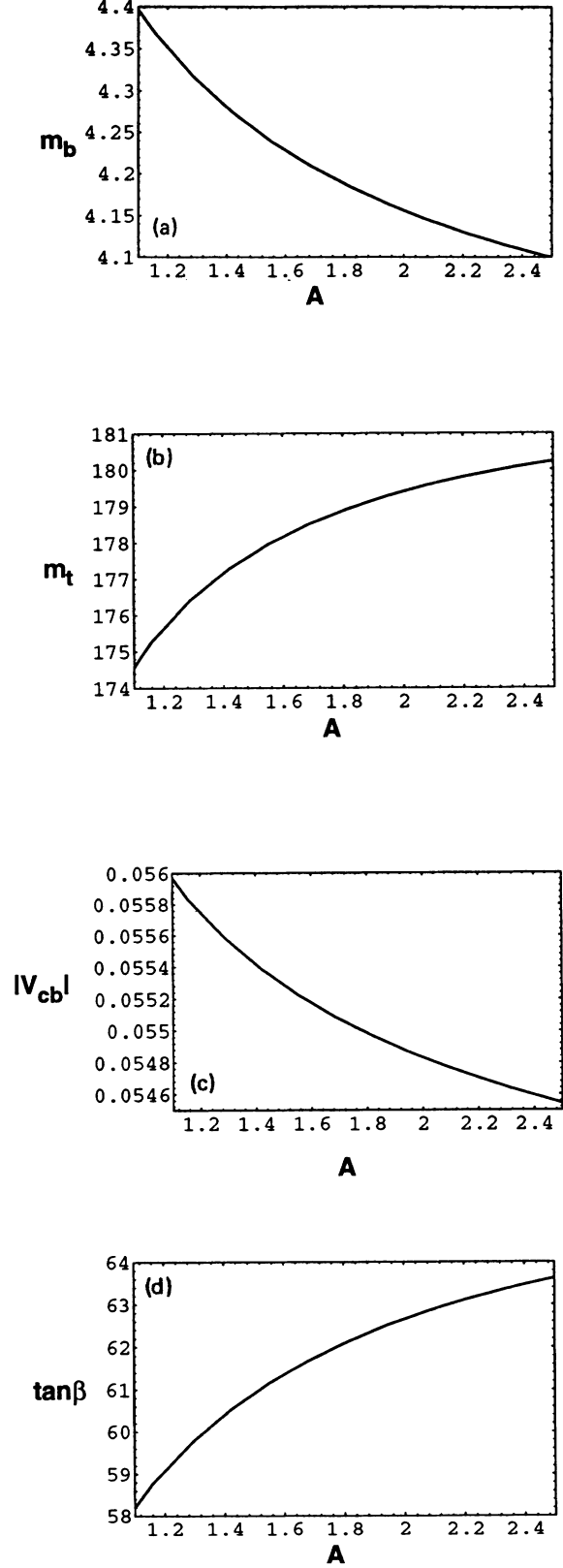


FIG. 7. For the case of $A \equiv \lambda_{t_U} = \lambda_{b_U} = \lambda_{\tau_U}$ in the MSSM with $M_S = 180$ GeV, $\alpha_{3c}(M_Z) = 0.121$, and threshold corrections having been ignored for simplicity, we plot running mass m_b , running mass m_t , $|V_{cb}|$, and $\tan\beta$ as a function of A in (a), (b), (c), and (d), respectively. In (c), we use $m_c = 1.22$ GeV.

TABLE III. Here we show how the three fermion $SO(10)$ gauge group spinor fields, three 126-dimensional representation Higgs fields, the 45-dimensional Higgs field, and the 210-dimensional Higgs field of our example model of Sec. VI transform under the model's softly broken three $U(1)$ symmetries.

$U(1)$	$\mathbf{16}_1$	$\mathbf{16}_2$	$\mathbf{16}_3$	$\mathbf{10}_1$	$\mathbf{10}_2$	$\mathbf{10}_3$	$\overline{\mathbf{126}}_1$	$\overline{\mathbf{126}}_2$	$\overline{\mathbf{126}}_3$	$\mathbf{45}$	$\mathbf{210}$
X	1	1	1	-2	-2	-2	-2	-2	-2	0	0
Y	2	1	0	-3	-1	0	4	-2	0	$-\frac{1}{2}$	$-\frac{1}{2}$
Z	1	0	0	-1	0	0	-2	0	0	-1	0

both of the couplings A and D from being too large. For example, when $m_b = 4.4 \text{ GeV}$, D can only be as small as 2.03 when $A = 1.02$, $m_t = 200 \text{ GeV}$, $\tan\beta = 74.9$, and $|V_{cb}|$ is 0.055 for $m_c = 1.22 \text{ GeV}$. A similar problem results if we increase M_I . We find that the unification of the bottom and τ Yukawa couplings is only feasible in the 2HSM when $M_I \ll M_U$ and $\alpha_{3c}(M_Z)$ is low, near 0.111.

VI. $U(1)^3$ SYMMETRY AND INDUCED VEV'S TO GIVE MASS MATRICES

Recently the authors of Ref. [18] have shown that if certain reasonable assumptions are made, then the neutrino mass ratios and leptonic mixing angles are completely determined by the 13 SM fermion sector parameters within the context of minimal $SO(10)$ grand unification. Their 13-parameter model is capable of generating all of the fermion masses and quark mixing angles and predicting the neutrino spectrum without depending upon any flavor symmetries. Crucial to their scheme is the observation that the electroweak breaking VEV of the $\mathbf{10}$ representation Higgs field will induce a small VEV in the superheavy bidoublet of the $\mathbf{126}$ representation Higgs field. Their model of course has little predictive ability in the SM sector.

In this section we give an example of a scheme that makes use of the idea of induced VEV's from superheavy fields, but at the same time limiting the structure of the mass matrices by using softly broken global symmetries. Specifically, we use $U(1)^3$ symmetry to generate mass matrices similar to Eq. (92) which account for the hierarchy of masses and mixing angles. We shall have to go beyond the minimal $SO(10)$ model to accomplish this.

We consider the possibility that $SO(10)$ gauge symmetry is broken to the gauge symmetry $\{2_L 2_R 4_C\}$ by a $\mathbf{210}$ representation Higgs field. At the next stage, symmetry is broken to $\{2_L 2_R 1_{B-L} 3_C\}$ by $\mathbf{210}$ as well as a $\mathbf{45}$ representation of Higgs field. Breaking to the SM is done by a $\mathbf{126}$ representation, and then finally the electroweak symmetry is broken by a complex $\mathbf{10}$ representation. In our example, we find that we need two superheavy $\mathbf{10}$ representations and two superheavy $\mathbf{126}$ fields. The superheavy fields have only very small induced VEV's. The $\mathbf{10}$ representation that does the electroweak symmetry breaking we will denote by $\mathbf{10}_3$, and the $\mathbf{126}$ representation Higgs field that breaks the symmetry $\{2_L 2_R 4_C\}$ to $\{2_L 2_R 1_{B-L} 3_C\}$ we will denote by $\mathbf{126}_3$. We show in Table III all the fields that we employ and their transformation properties under three different $U(1)$ symmetries $U(1)_X$, $U(1)_Y$, and $U(1)_Z$. All bidoublets are superheavy

except that of the $\mathbf{10}_3$ field. The operators that give the fermion masses are shown in Fig. 8. These operators give the Yukawa matrices

$$\mathbf{U} = \begin{pmatrix} 0 & C & 0 \\ C & E & B \\ 0 & B & A + a \end{pmatrix},$$

$$\mathbf{D} = \begin{pmatrix} 0 & Cr_C & 0 \\ Cr_C & Er_E & Br_B \\ 0 & Br_B & Ar_A + ar_a \end{pmatrix}, \quad (114)$$

$$\mathbf{E} = \begin{pmatrix} 0 & Cr_C & 0 \\ Cr_C & -3Er_E & Br_B \\ 0 & Br_B & Ar_A - 3ar_a \end{pmatrix},$$

where the r_i 's are ratios of the "down" VEV's to the "up" VEV's in the operators. These Yukawa matrices go to those of our SM case in the limit of small r_B and r_E large compared to 3.

It is pointed out in Ref. [9] that a fourfold symmetrized product of the $\mathbf{126}$ -dimensional representation is an $SO(10)$ singlet. Hence terms in the Lagrangian such as $\lambda(\mathbf{126}_i)_5^4$ will explicitly break a $U(1)$ symmetry to discrete symmetry if $\mathbf{126}_i$ has a $U(1)$ charge. We can use the term $\lambda(\mathbf{126}_1)_5^4$ to break $U(1)$ quantum numbers

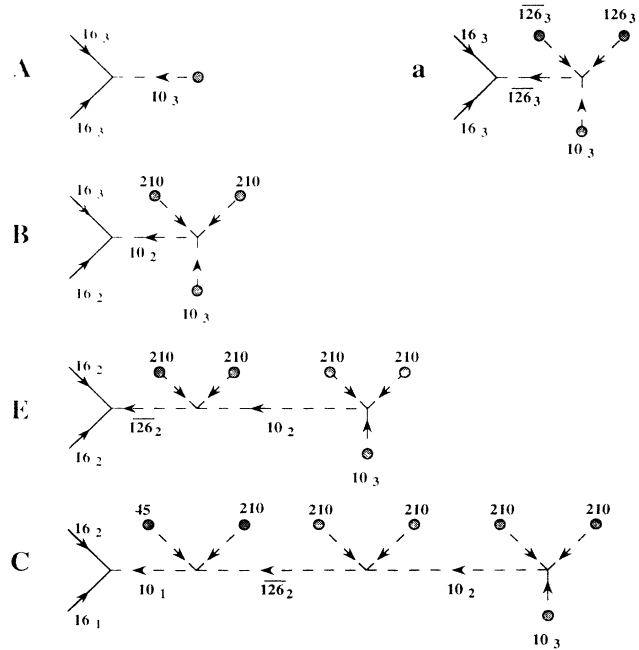


FIG. 8. In this figure we show the operators discussed in Sec. VI that give the Yukawa couplings of Eq. (114) from the fields given in Table III.

X , Y , and Z to a mod 8, a mod 16, and a mod 8 discrete symmetry, respectively, and avoid massless Nambu-Goldstone bosons.

We note that in this scheme one cannot determine the neutrino sector without making further assumptions. However, we still should check to see if the scheme is capable of generating low mass neutrinos and leptonic mixing angles that are in a range to provide an explanation for the observed solar neutrino deficit via neutrino oscillation. Our scheme provides a Majorana mass matrix with three unknown couplings to the three $\overline{126}$ representation Higgs fields and which is of the form

$$M_{NN} = \begin{pmatrix} \beta & 0 & 0 \\ 0 & \alpha & 0 \\ 0 & 0 & 1 \end{pmatrix} V, \quad (115)$$

where $V \sim M_R$ and α and β are in general complex and may be assumed to be small. We assume the $(1, 3, 10)$ submultiplets, given in $\{2_L 2_R 4_C\}$ notation, of the fields $\mathbf{126}_2$ and $\mathbf{126}_1$ have masses near the unification scale, and that they acquire small VEV's. We do not explain these small VEV's, but we note that they could result from a more complicated Higgs structure. The neutrino Dirac mass matrix at M_U is approximately the same as $U\kappa$. We find that it is possible to get the neutrino spectrum into the previously mentioned small-angle adiabatic solution window, $\Delta m^2 \simeq (0.3-1.2) \times 10^{-5} \text{ eV}^2$ and $\sin^2 \theta_{e\mu} \simeq (0.4-1.5) \times 10^{-2}$, when $|\alpha| \ll 1$ and $|\beta| \ll |\alpha|$ provided we give phases to the SM singlet VEV's. For example, if we assume the phases are zero and use $\alpha = 0.005$ and $\beta = \alpha^2$ for when $|V_{cb}| = 0.05$ we get $m_{\nu_\tau}/m_{\nu_\mu} \approx 500$ and $\sin^2 \theta_{e\mu} \approx 0.018$. However, for example, if we give a complex phase of ϕ , 2ϕ , and 0 to the third-, second-, and first-generation diagonal entries in the Majorana mass matrix, then for $|V_{cb}| = 0.05$ we get $m_{\nu_\tau}/m_{\nu_\mu} \approx 750$ and $\sin^2 \theta_{e\mu} \approx 0.01$, which is an acceptable solution to the solar neutrino problem.

VII. SUMMARY AND CONCLUSIONS

In this paper, we have examined the predictive ability of fermion mass *Ansätze* in non-SUSY SO(10) grand unification in contrast to SUSY SO(10) since there is still no direct evidence for SUSY. We have considered the two possibilities that between the scale of the top mass and the scale M_I the effective theory is the SM and that it is the 2HSM. We have compared these cases to the case where between the scale of the top mass and M_U the effective theory is the MSSM, where the maximal SM parameter predictive ability is six parameters with $|V_{cb}|$ a little large or five parameters all within 1σ experimental limits. We have not considered *Ansätze* such as given in Ref. [11] where certain relations are assumed between all of the entries of the up and down quark Yukawa matrices

with the result of the predictive ability being improved.

In the SM case, we find that condition $m_b = m_\tau$ at the unification scale M_U is impossible to maintain with $m_t^{\text{pole}} \geq 130 \text{ GeV}$ and $m_b^{\text{pole}} < 5 \text{ GeV}$. Nevertheless, we are able to predict five SM parameters to be within their 1σ experimental limits. Specifically, m_t is in the range of about 150–180 GeV for $|V_{cb}|$ in the upper half of its 1σ range. This is shown in Fig. 3(a) and Fig. 4(a) for the case of $M_I \sim 10^{11} \text{ GeV}$ and $M_I \sim 10^{14} \text{ GeV}$ respectively. The results for the MSSM are quite similar for the ranges of m_t and $|V_{cb}|$ that are permissible. The values of $|V_{ub}/V_{cb}|$, m_s , and J for the SM and the MSSM cases are shown in Table II. As can be seen they are quite similar and lie within the 1σ experimental limits. These three parameters are found to depend somewhat on the scale at which the Pati-Salam group is broken. The predictions for these three parameters increase when the intermediate scale M_I is increased. In all cases $|V_{ub}/V_{cb}|$ is seen to be on the lower end of its acceptable range. For the SM case with $M_I \sim 10^{11} \text{ GeV}$, $|V_{ub}/V_{cb}|$ must be less than about 0.062, while in the SM case with $M_I \sim 10^{14} \text{ GeV}$ it can be as high as about 0.066. As usual, the prediction for m_s/m_d only depends on m_μ/m_e and is found to be 24.73, within experimental bounds.

As in the MSSM and unlike in the SM, in the 2HSM both $m_b = m_\tau$ and with large $\tan\beta$ unification of the top, bottom, and τ Yukawa couplings at the gauge unification scale are possible. We find we can predict $\tan\beta$ and six SM parameters for the case where the top, bottom, and τ Yukawa couplings are unified at high energies. This is found only to work when $\alpha_{3c}(M_Z)$ is near 0.111, and so could be ruled out with better experimental determination of $\alpha_{3c}(M_Z)$. The predictions for the four parameters m_s/m_d , $|V_{ub}/V_{cb}|$, m_s , and J are essentially the same as for the SM. However, as shown in Fig. 6(a), $|V_{cb}|$ is predicted to be above its 1σ limits. In fact, only for m_t above 180 GeV is $|V_{cb}|$ within its 90% confidence limits. Of course, by adding another parameter to the *Ansatz* and decreasing its number of predictions by 1 $|V_{cb}|$ may be allowed to be in its 1σ range. However, from comparison of Fig. 6(a) and Fig. 6(b) one can see that for m_t to be less than 180 GeV, the running mass m_b must be greater than 4.4 GeV. On the other hand, if we give up the unification of the top and bottom Yukawa couplings but retain $m_b = m_\tau$ above M_I , then it is possible for the top pole mass to be below 180 GeV. In this case, $|V_{cb}|$ lies above its 1σ limits but within its 90% confidence limits. The predictions for m_s/m_d , $|V_{ub}/V_{cb}|$, m_s , and J are essentially unchanged.

ACKNOWLEDGMENTS

This work has been supported by the Department of Energy, Grant No. DE-FG06-85ER-40224.

- [1] S. Dimopoulos, L. J. Hall, and S. Raby, Phys. Rev. Lett. **68**, 984 (1992); Phys. Rev. D **45**, 4192 (1992).
 [2] G. Anderson, S. Dimopoulos, L. J. Hall, S. Raby, and G. D. Starkman, Phys. Rev. D **47**, R3702 (1993).

- [3] V. Barger, M. S. Berger, and P. Ohmann, Phys. Rev. D **47**, 1093 (1993).
 [4] V. Barger, M. S. Berger, T. Han, and M. Zralek, Phys. Rev. Lett. **68**, 984 (1992); K. S. Babu and Q. Shafi, Phys.

- Rev. D **47**, 5004 (1993); Bartol Report No. BA-93-09 (unpublished); H. Arason, D. J. Castaño, E. J. Piard, and P. Ramond, Phys. Rev. D **47**, 232 (1993); P. Ramond, R. G. Roberts, and G. G. Ross, Institute for Fundamental Theory Report No. UFIFT-(RAL-93-010 or -HEP-93-06) (unpublished).
- [5] H. Fritzsch, Phys. Lett. **70B**, 436 (1977); **73B**, 317 (1978); Nucl. Phys. **B155**, 189 (1979).
- [6] H. Georgi and C. Jarlskog, Phys. Lett. **86B**, 297 (1979).
- [7] R. Gatto, G. Sartori, and M. Tonin, Phys. Lett. **28B**, 128 (1968); N. Cabibbo and L. Maiani, *ibid.* **28B**, 131 (1968); R. J. Oakes, *ibid.* **29B**, 683 (1969); S. Weinberg, *A Festschrift for I. I. Rabi*, Transactions of the New York Academy of Sciences (1977); F. Wilczek and A. Zee, Phys. Lett. **70B**, 418 (1977).
- [8] E. Ma, Phys. Rev. D **43**, R2761 (1991); F. J. Gilman and Y. Nir, Annu. Rev. Nucl. Part. Sci. **40**, 213 (1990); X. G. He and W. S. Hou, Phys. Rev. D **41**, 1517 (1990).
- [9] J. Harvey, P. Ramond, and D. B. Reiss, Phys. Lett. **92B**, 309 (1980); Nucl. Phys. **B199**, 223 (1982).
- [10] H. Georgi, in *Particles and Fields—1974 (APS/DPF Williamsburgh)*, Proceedings of the 1974 Meeting of the APS Division of Particles and Fields, edited by C. E. Carlson, AIP Conf. Proc. No. 23 (AIP, New York, 1975); H. Fritzsch and P. Minkowski, Ann. Phys. (N.Y.) **93**, 193 (1975).
- [11] G. Anderson, S. Dimopolous, L. J. Hall, S. Raby, and G. D. Starkman, Phys. Rev. D **49**, 3660 (1994).
- [12] Originally the weak mixing angle was predicted in the following sources: H. Georgi, H. Quinn, and S. Weinberg, Phys. Rev. Lett. **33**, 451 (1974); S. Dimopolous, S. Raby, and F. Wilczek, Phys. Rev. D **24**, 1681 (1981); S. Dimopolous and H. Georgi, Nucl. Phys. **B193**, 150 (1981). With the recent data from the CERN e^+e^- collider LEP the possibility of coupling unification in the MSSM was demonstrated in the following sources: U. Amaldi, W. de Boer, and H. Fürstenau, Phys. Lett. B **260**, 447 (1991); P. Langacker and M. Luo, Phys. Rev. D **44**, 817 (1991).
- [13] F. del Aguila and L. Ibañez, Nucl. Phys. **B177**, 60 (1981); R. N. Mohapatra and G. Senjanović, Phys. Rev. D **27**, 1601 (1983).
- [14] N. G. Deshpande, E. Keith, and P. B. Pal, Phys. Rev. D **46**, 2261 (1992); D. Chang, R. N. Mohapatra, J. M. Gipson, R. E. Marshak, and M. K. Parida, *ibid.* **31**, 1718 (1985); J. M. Gipson and R. E. Marshak, *ibid.* **31**, 1705 (1985); Y. Tosa, *ibid.* **28**, 1731 (1983); P. Langacker and M. Luo, *ibid.* **44**, 817 (1991).
- [15] R. N. Mohapatra and M. K. Parida, Phys. Rev. D **47**, 264 (1993).
- [16] L. Lavoura and L. Wolfenstein, Phys. Rev. D **48**, 264 (1993).
- [17] D. Chang, R. N. Mohapatra, and K. Parida, Phys. Lett. **142B**, 55 (1984); Phys. Rev. Lett. **52**, 1072 (1984); Phys. Rev. D **30**, 1052 (1984).
- [18] K. S. Babu and R. N. Mohapatra, Phys. Rev. Lett. **70**, 2845 (1993).
- [19] K. Inoue, A. Kakuto, H. Komatsu, and S. Takeshita, Prog. Theor. Phys. **67**, 1889 (1982); T. P. Cheng, E. Eichten, and L-F. Li, Phys. Rev. D **9**, 2259 (1974).
- [20] D. R. T. Jones, Phys. Rev. D **25**, 581 (1982); M. B. Einhorn and D. R. T. Jones, Nucl. Phys. **B196**, 475 (1982); M. E. Machacek and M. T. Vaughn, *ibid.* **B222**, 83 (1983); L. J. Hall, *ibid.* **B178**, 75 (1981).
- [21] See talks by S. C. C. Ting, R. K. Ellis, and W. J. Marciano, in *The Fermilab Meeting*, Proceedings of the Annual Meeting of the Division of Particles and Fields of the APS, Batavia, Illinois, 1992, edited by C. Albright *et al.* (World Scientific, Singapore, 1993).
- [22] O. V. Tarasov, A. A. Vladimirov, and A. Y. Zharkov, Phys. Lett. **93B**, 429 (1980); S. G. Gorishny, A. L. Kateav, and S. A. Larin, Yad. Fiz. **40**, 517 (1984) [Sov. J. Nucl. Phys. **40**, 329 (1984)]; S. G. Gorishny *et al.*, Mod. Phys. Lett. A **5**, 2703 (1990).
- [23] E. Ma and S. Pakvasa, Phys. Lett. **86B**, 43 (1979); Phys. Rev. D **20**, 2899 (1979); K. S. Babu, Z. Phys. C **35**, 69 (1987); K. Sasaki, *ibid.* **32**, 149 (1986); B. Grzadkowski, M. Linder, and S. Theisen, Phys. Lett. B **198**, 64 (1987); M. Olechowski and S. Pokorski, *ibid.* **257**, 388 (1991); V. Barger, M. Berger, and P. Ohmann, Phys. Rev. D **47**, 2038 (1993); K. S. Babu and Q. Shafi, *ibid.* **47**, 5004 (1993).
- [24] S. G. Naculich, Phys. Rev. D **48**, 5293 (1993).
- [25] B. Pendleton and G. G. Ross, Phys. Lett. **98B**, 291 (1981); C. T. Hill, Phys. Rev. D **24**, 691 (1981).
- [26] G. Altarelli, in *Proceedings of the International Europhysics Conference on High Energy Physics*, Marseille, France, 1993, edited by J. Carr and M. Perottet (Editions Frontières, Gif-sur-Yvette, 1993); J. L. Lopez, D. V. Nanopoulos, G. Park, X. Wang, and A. Zichichi, Texas A&M University Report No. CTP-TAMU-74/93 (unpublished).
- [27] E. M. Freire, Phys. Rev. D **27**, 209 (1990).
- [28] E. M. Freire, G. Lazarides, and Q. Shafi, Mod. Phys. Lett. A **5**, 2453 (1990).
- [29] The running masses for quarks are given in J. Gasser and H. Leutwyler, Phys. Rep. **87**, 77 (1982); constraints from chiral-Lagrangian analysis on the ratios m_u/m_d and m_s/m_d are given in D. Kaplan and A. Manohar, Phys. Rev. Lett. **56**, 2004 (1986) and in H. Leutwyler, Nucl. Phys. **B337**, 108 (1990); limits on the weak mixing angles are found in Particle Data Group, J. J. Hernández *et al.*, Phys. Lett. B **239**, 1 (1990).
- [30] S. Dimopolous, L. Hall, and S. Raby, Phys. Rev. D **46**, R4793 (1992).
- [31] S. Abachi *et al.*, Phys. Rev. Lett. **72**, 2138 (1994).
- [32] S. Dimopolous, L. Hall, and S. Raby, Phys. Rev. D **47**, R3697 (1992).
- [33] X. Shi, D. N. Schramm, and J. Bahcall, Phys. Rev. Lett. **69**, 717 (1992); S. A. Bludman, N. Hata, D. C. Kennedy, and P. Langacker, Phys. Rev. D **47**, 2220 (1993).